AN INVESTIGATION INTO THE EFFECTS OF ALLOSTERIC MODULATORS OF THE HUMAN 5-HT$_{3A}$ RECEPTOR

BY JOSEPHINE C. PALANDRI

UNIVERSITY^{OF}
BIRMINGHAM

A thesis submitted to the University of Birmingham for the degree of MASTER OF SCIENCE BY RESEARCH

Pharmacy, Pharmacology & Therapeutics

School of Clinical & Experimental Medicine

College of Medical & Dental Sciences

University of Birmingham

December 2014

TABLE OF FIGURES

ABSTRACT

The 5-HT$_{3A}$ receptor is a cys-loop ligand gated ion channel re-emerging as an attractive target in irritable bowel syndrome (IBS), which currently affects 5-10% of the global population. At present, IBS therapies involve the complete blockade of the 5-HT$_{3A}$ receptor by orthosteric antagonists, which leads to complications such as severe constipation and ischaemic colitis. Allosteric modulation could bypass such side effects, as receptor function relies upon the endogenous neurotransmitter to retain physiological control. Here, we investigate the structure and function of the 5-HT$_{3A}$ receptor allosteric binding site by the identification of novel allosteric compounds and the generation of an α7/5-HT$_{3A}$ chimeric receptor. Intracellular calcium assays and competitive radioligand binding experiments indicated that the halogenated indole derivatives, 5-chloroindole (5-Cl) (Newman et al., 2013) and 5-(trifluoromethyl)indole (5-TFMI) are positive allosteric modulators (PAM) of the 5-HT$_{3A}$ receptor; however 5-TFMI also displayed a degree of orthosteric binding. The structural analogues, 5-bromoindazole (5-BI) and 5-bromo-benzimidazole (5-BBI) exhibited contrasting effects, by potentiating and decreasing 5-HT-evoked responses, respectively. Further studies suggested some orthosteric binding by 5-BI and 5-BBI at high concentrations. The allosteric binding site for 5-Cl was previously located in the N-terminus of the mouse 5-HT$_{3A}$ receptor. To identify the site in the human receptor, we attempted to construct a human chimeric α7V$_{201}$5-HT$_{3A}$ receptor to allow further investigation into this question. Our data suggest these halogenated indoles are allosteric compounds and, when studied in combination with the α7V$_{201}$5-HT$_{3A}$ chimera, could identify the required core structure of high affinity compounds needed for negative allosteric modulation in the treatment of IBS.

ACKNOWLEDGEMENTS

PUBLICATIONS ARISING FROM RESEARCH

Palandri J.C., Butterworth S., Grafton G., Barnes N.M., 2013. [Abstract] Allosteric Modulation of the Human 5-HT$_3$A receptor by 5-(trifluoromethyl)-indole. (Poster presented at *Pharmacology 2013*)

Grafton G., Myerson R., Palandri J.C., Weller M.D., Simpkins N.S., Butterworth S., Barnes N.M., 2014. [Abstract] Negative Allosteric Modulation of the Human 5-HT3A receptor ; Stategy for the Treatment of Irritable Bowel Syndrome. *11th Congress of the International Society for Serotonin Research*

CHAPTER 1: INTRODUCTION

1.1. The Serotonergic System

5-hydroxytryptamine (5-HT), or serotonin, is a monoamine neurotransmitter involved in multiple signalling pathways throughout various physiological systems. 5-HT was initially identified as a potent vasoconstrictor in serum (Rapport et al, 1947) and the notion of 5-HT binding to specific receptors in the nervous system and on smooth muscle was introduced in the 1950s, by Gaddum et al (1953).

1.2. Distribution of 5-HT

1.2.1. Blood

5-HT was initially identified in the 1940s as a potent vasoconstrictor originating from platelets in the serum (Rapport, 1947). Platelets accumulate 5-HT by active uptake and release it when aggregated at sites of tissue damage, possibly to help recruit further platelets (Hardisty (1955), Vanhoutte (1991)).

1.2.2. CNS

5-HT in the brain is synthesised from L-tryptophan and stored in vesicles in serotonergic neurons located mainly in the raphe nuclei of the midbrain. These neurons project to almost every region of the brain, including the hippocampus, cerebellum, midbrain, cortex, as well as the spinal cord (Murphy, 1998). 5-HT is released from axon terminals, and signalling is

terminated by reuptake into the presynaptic terminal by an energy-dependent transporter molecule, the serotonin transporter (SERT). Due to release of 5-HT in almost every region of the CNS, the serotonergic system is involved in regulating a variety of functions such as: blood pressure, body temperature, appetite, hormone release and emotional behaviour. Imbalances of 5-HT signalling can therefore disrupt these functions and play a role in the pathophysiology of hypertension, hormonal dysfunction, anxiety and depression.

1.2.3. Periphery

Approximately 90-95% of all 5-HT is stored within and secreted by enterochromaffin cells in the gut. Epithelial enterochromaffin cells act as sensory transducers that activate the mucosal processes of both intrinsic and extrinsic primary afferent neurones through their release of 5-HT. The primary afferent neurons are present in both the submucosal and myenteric plexus, and stimulate secretory and peristaltic reflexes when activated (Gershon and Tack, 2007). As a neurotransmitter in the gut, 5-HT can also stimulate cholinergic neurons to release acetylcholine resulting in smooth muscle contraction, or it can stimulate inhibitory neurons to release nitric oxide, mediating smooth muscle relaxation (Sikander et al., 2009).

1.3. Pathophysiology of the Serotonergic System

Associated with its widespread distribution, 5-HT is involved in regulating a range of central and peripheral functions; therefore misregulation of 5-HT signalling can have multiple adverse effects throughout the body. 5-HT has been found to play a role in anxiety, depression, addiction and emesis by various mechanisms including excessive release of 5-HT,

lack of reuptake by the serotonin transporter (SERT) or lack of metabolism to terminate signalling [for reviews see (Barnes and Sharp, 1999, Filip and Bader, 2009)].

In the periphery, 5-HT has been shown to mediate some of the symptoms of irritable bowel syndrome (IBS). Increased postprandial plasma 5-HT levels were detected in patients with IBS, which correlates to colonic motility (Houghton et al., 2007) resulting in diarrhoea. Mouse knock-out models of SERT exhibit increased colonic motility, watery stools and alternating patterns of constipation and diarrhea, similar to the symptoms of IBS (Chen et al., 2001).

1.4.   Receptor Classification

There are 14 known genetically and pharmacologically distinct 5-HT receptors classed into 7 families (5-HT_1 to 5-HT_7) (Langer et al., 1980, Hoyer et al., 1994, Barnes and Sharp, 1999) Most of the 5-HT receptors have been identified as seven transmembrane domain G protein coupled receptors, except for the 5-HT_3 receptors, which are cys-loop ligand-gated ion channels.

1.4.1. The 5-HT_1 Receptor Family

The 5-HT_1 receptor family is comprised of five receptor subtypes: 5-HT_{1A}, 5-HT_{1B}, 5-HT_{1D}, 5-ht_{1E} and 5-ht_{1F}. The latter two subtypes are named in lower case as their presence has not yet been determined in native tissues. These receptors are seven transmembrane spanning proteins negatively coupled to adenylate cyclase via the αi G protein.

1.4.1.1.   5-HT$_{1A}$ Receptor

The gene coding for the human 5-HT$_{1A}$ receptor is localised on chromosome 5 (5q11.2-q13) and codes for a seven transmembrane spanning protein with sites for glycosylation and phosphorylation.

Distribution of this receptor has been determined by autoradiography using a range of radioligands such as [^{3}H]-5-HT and [^{3}H]-8-OH-DPAT (Pazos and Palacios, 1985). 5-HT$_{1A}$ receptors are mainly found in limbic brain areas such as the hippocampus (postsynaptically), lateral septum, cortex and mesencephalic raphe nuclei (presynaptically).

The 5-HT$_{1A}$ receptor exerts inhibitory actions by coupling to the αi G protein in rat and guinea pig hippocampus. In electrophysiological studies, 5-HT$_{1A}$ receptor activation causes neuronal hyperpolarisation, exerted by potassium (K$^+$) channel opening. Activation of these receptors mediates various physiological and behavioural effects, such as neuroendocrine regulation of adrenocorticotrophic hormone (ACTH) (Jørgensen et al., 2001). In murine 5-HT$_{1A}$ receptor knock-out models, mice showed increased levels of anxiety in the elevated plus maze and decreased baseline immobility in tail suspension tests (Heisler et al., 1998). Presynaptic 5HT$_{1A}$ agonists, such as buspirone, are being used for the treatment of anxiety and depression by attenuating 5-HT neurotransmission in the raphe nuclei (Tunnicliff, 1991).

1.4.1.2.   5-HT$_{1B}$ Receptor

The 5-HT$_{1B}$ receptor was found to be pharmacologically different to the 5-HT$_{1A}$ receptor, with a lower affinity for [^{3}H]-8-OH-DPAT in autoradiographic studies (Middlemiss and Fozard, 1983). The gene encoding for the 5-HT$_{1B}$ receptor is located on chromosome 6q13 (Saudou and Hen, 1994).

5-HT$_{1B}$ receptors are expressed in the CNS, particularly in basal ganglia, striatum and frontal cortex. They are thought to be presynaptic autoreceptors and potentially as heteroreceptors modulating the release of other neurotransmitters such as acetylcholine, glutamate and dopamine (Hoyer et al., 2002, Pauwels, 1997). These receptors are also found on cerebral arteries and other vascular tissues, and are thought to play a role in migraines. Agonists such as sumatriptan have been developed to treat acute migraines.

1.4.1.3.   5-HT$_{1D}$ Receptor

The gene coding for the 5-HT$_{1D}$ receptor is located on chromosome 1p34.3–p36.3. This receptor possesses 63% structural homology with the 5-HT$_{1B}$ receptor, and was once thought to be species a homologue (Hoyer and Middlemiss, 1989). Novel 5-HT$_{1B}$ receptor ligands have suggested the presence of 5-HT$_{1D}$ autoreceptors in the dorsal raphe nuclei (Roberts et al., 2001), and also in the human heart. PNU 109291, a selective 5-HT$_{1D}$ agonist, has been shown to suppress meningeal neurogenic inflammation and trigeminal nociception in guinea pig models, suggesting this receptor could be a potential therapeutic target for migraine (Cutrer et al., 1999).

1.4.1.4.   5-ht$_{1E}$ Receptor

The gene for the 5-ht$_{1E}$ receptor has been located on human chromosome 6q14-q15 (Levy et al., 1994). Radioligand binding studies revealed a low affinity binding site with different pharmacology to the 5-HT$_{1D}$ receptor, suggesting a novel 5-HT receptor. However, due to the lack of specific radioligands to the 5-ht$_{1E}$ receptor, distribution, pharmacology and physiological function of this receptor have not been characterised in humans.

1.4.1.5. 5-ht$_{1F}$ Receptor

The human 5-ht$_{1F}$ receptor gene is located on chromosome 3q11 (Saudou and Hen, 1994). 5-ht$_{1F}$ mRNA was first localised in the mouse and guinea pig brain using in situ hybridisation in the hippocampus (CA1–CA3 cell layers), cortex and dorsal raphe nucleus (Bruinvels et al., 1994). Similarly to the 5-ht$_{1E}$ receptor, activation of the native human 5-ht$_{1F}$ receptor has unknown effects, but based on the anatomical location; it has been hypothesised that they could play a role in visual and cognitive function and as 5-HT autoreceptors.

1.4.2. The 5-HT$_2$ Receptor Family

There are three receptor subtypes in the 5-HT$_2$ receptor family: 5-HT$_{2A}$, 5-HT$_{2B}$ and 5-HT$_{2C}$. These receptors are seven transmembrane-spanning proteins, all positively coupled to phospholipase C and mobilise intracellular calcium via G$_{q/11}$.

1.4.2.1. 5-HT$_{2A}$ Receptor

The 5-HT$_{2A}$ receptor gene is located on human chromosome 13q14-q21 (Chen et al., 1992). Autoradiography, in situ hybridisation and immunocytochemistry have localised 5-HT$_{2A}$ receptors to many forebrain regions, but particularly cortical areas (neocortex, entorhinal and pyriform cortex, claustrum), caudate nucleus, nucleus accumbens, olfactory tubercle and hippocampus (Lopez-Gimenez et al., 1997). There is an interest in targeting the 5-HT$_{2A}$ receptor with antipsychotic drugs due to it playing a role in hallucinogenic mechanisms (Glennon, 1990). It has also been found to mediate responses such as hyperthermia (Gudelsky et al., 1986) and neuroendocrine responses.

1.4.2.2.   5-HT$_{2B}$ Receptor

The human 5-HT$_{2B}$ receptor gene is located at chromosomal position 2q36.3–2q37.1. 5-HT$_{2B}$ mRNA transcripts have been detected in human liver and kidney and in low levels in the brain (Bonhaus et al., 1995). Little is known about the function of the native 5-HT$_{2B}$ receptor, although the 5-HT$_{2B}$ receptor agonist BW 723C86 has been shown to have anxiolytic effect in rat models (Kennett et al., 1996).

1.4.2.3.   5-HT$_{2C}$ Receptor

The 5-HT$_{2C}$ receptor gene is X-linked, located on chromosome Xq24 (Xie et al., 1996). There is little evidence to suggest the 5-HT$_{2C}$ receptor is expressed in other tissues than the brain. Very high levels of 5-HT$_{2C}$ binding sites were detected in the choroid plexus (Conn et al., 1986), but also in areas of the cortex, limbic system, and basal ganglia (Sheldon and Aghajanian, 1991). Activation of 5-HT$_{2C}$ receptors mediates a variety of behavioural responses such as hypolocomotion, hypophagia and anxiety, and are also possibly implicated in the pathophysiology of schizophrenia and depression (Koek et al., 1992).

1.4.3. 5-HT$_4$ Receptor

The gene encoding for the 5-HT$_4$ receptor was mapped to chromosome 5q31-33 (Claeysen et al., 1997), and several isoforms and splice variants have been identified. 5-HT$_4$ receptors are 7-transmembrane spanning proteins positively coupled to adenylate cyclase. The receptors are distributed throughout tissues such as the gut (Blondel et al., 1998), where they mediate peristalsis and secretory responses, in cardiac atria, where they mediate tachycardia in the

right atria and positive inotropic effects in the left atria; and the brain, enhancing cognition (Mialet et al., 2000).

1.4.4. 5-HT$_5$ Receptors

The 5-HT$_5$ receptors are the least well understood receptors of all the subtypes. Two subtypes of the receptor (5-ht$_{5A}$ and 5-ht$_{5B}$) have been found in rodents and the genes encoding the human subtypes have been located on chromosomes 7q36.1 (Schanen et al., 1996)and 2q11-13 respectively, although the gene encoding the 5-ht$_{5B}$ subunit failed to encode a functional receptor (Grailhe et al., 2001). Recently, Goodfellow et al. (2012) characterised functional 5-HT$_{5A}$ receptors in the rodent prefrontal cortex, by electrophysiology. They showed activation of 5-HT$_{5A}$ receptors produces small inwardly-rectifying K$^+$ currents, and knock-out of the *htr5A* gene caused a compensatory increase in 5-HT$_{1A}$ receptor expression, suggesting a possible role in anxiety and depression modulation.

1.4.5. 5-HT$_6$ Receptors

The gene coding for the 5-ht$_6$ receptor sequence has been mapped to chromosome 1p35-36 (Kohen et al., 1996), and found to positively couple to adenylyl cyclase via G$_s$. Human 5-ht$_6$ mRNA has been located mostly postsynaptically throughout the central nervous system (Ruat et al., 1993), though low levels of mRNA have also been detected in the stomach and adrenal glands (Monsma et al., 1993). Antipsychotic drugs such as clozapine and olanzapine, and antidepressants such as clomipramine and amitriptyline act as 5-ht$_6$ antagonists suggesting their involvement in the clinical efficacy and/or the side effects associated with these drugs (Monsma et al., 1993, Kohen et al., 1996). Sleight et al. (1998) demonstrated an interaction between 5-ht$_6$ receptors and the central cholinergic system, as antagonists appear to increase

cholinergic transmission, with positive effects on learning and memory (Meneses et al., 2007), suggesting a potential target for cognitive disorders such as Alzheimer's disease.

1.4.6. 5-HT$_7$ Receptors

The gene encoding the 5-HT$_7$ receptor sequence has been mapped to chromosome 10q21-24 (Gelernter et al., 1995). Functional studies have shown that this receptor positively couples to adenylyl cyclase via G$_s$, is extensively distributed throughout vascular tissue and is responsible for the vasodilator in response to 5-HT in anaesthetised animals (Martin and Humphrey, 1994). It is also expressed in non-vascular smooth muscle and the CNS (Carter et al., 1995, Stowe and Barnes, 1998). Centrally, the 5-HT$_7$ receptor is thought to mediate a variety of functions such as the regulation of circadian rhythms (Lovenberg et al., 1993), manifestation of seizures (Bourson et al., 1997) and possible involvement in depressive behaviours (Guscott et al., 2005).

1.5. The 5-HT$_3$ Receptor Family

The 5-HT$_3$ receptors are the distinct from the other 5-HT receptors as they belong to the cys-loop ligand gated ion channel superfamily, which encompasses receptors such as the nicotinic acetylcholine receptors and GABA$_A$ receptors. They were originally discovered in the ileum and named M receptors by Gaddum and Picarelli (1957), due to their being blocked by morphine. A reclassification of serotonin receptors renamed the M receptor to 5-HT$_3$ (Bradley et al., 1986). Selective 5-HT$_3$ antagonists such as GR38032F (ondansetron) and BRL43694 (granisetron) revealed an anti-emetic effect of these compound and also helped in identifying the widespread presence of 5-HT$_3$ binding sites in the PNS (Miner and Sanger, 1986, Fozard,

1984). The presence of central 5-HT$_3$ binding sites was established using radioligand binding (Kilpatrick et al., 1987), and single channel studies confirmed the 5-HT3 receptors were ligand-gated ion channels (Derkach et al., 1989).

1.5.1. 5-HT$_3$ Receptor Structure

The functional 5-HT$_3$ receptor is a pentameric formation of either identical or non-identical subunits, which surround a central pore. Each subunit is formed of a large extracellular N-terminus, which contains the ligand binding site, 4 membrane-spanning regions termed M1-M4, which allow ion selectivity, a large intracellular loop between M3 and M4 and a small extracellular C-terminus. Several subunits have been identified: 5-HT$_{3A}$ and 5-HT$_{3B}$, 5-HT$_{3C}$, 5-HT$_{3D}$ and 5-HT$_{3E}$. Only the 5-HT$_{3A}$ subunit is able to form functional homomeric receptors, whilst the others appear to require at least one 5-HT$_{3A}$ subunit to form functional heteromeric receptors (Niesler et al., 2008). Figure 1 shows the diagrammatic representation of the structure of the 5-HT$_3$ receptors.
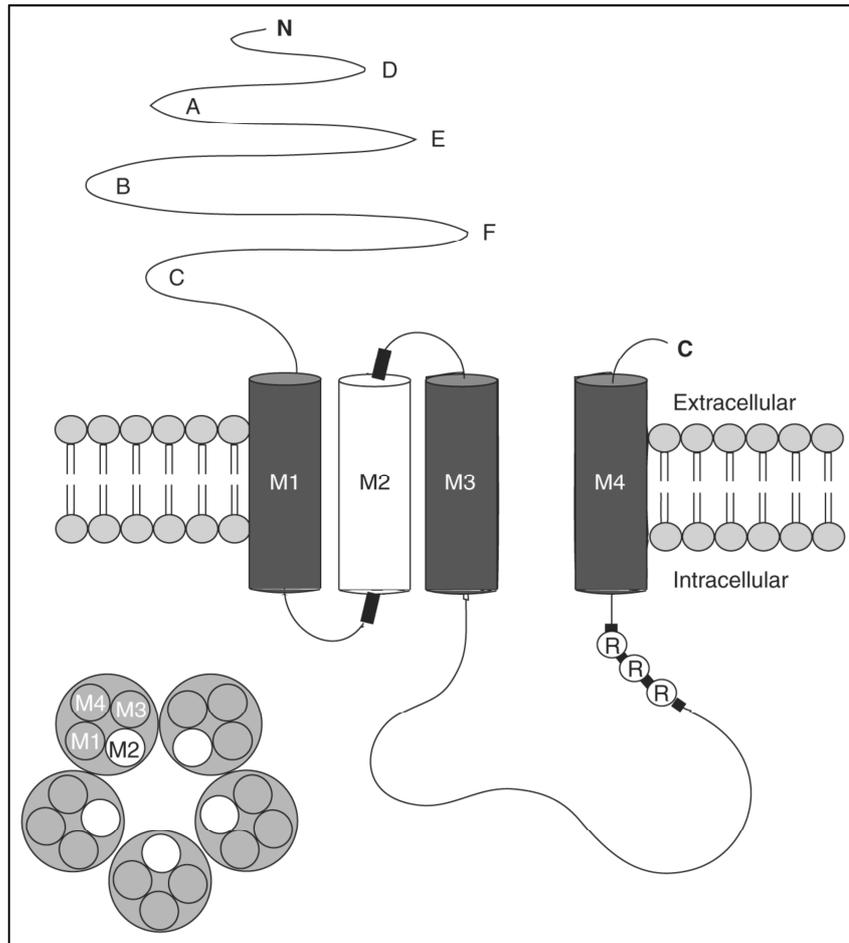
Figure 1: **Top**: Diagram of the structure of one subunit of the 5-HT$_3$ receptor as seen parallel to the plane of the membrane. The extracellular N-terminus, C-terminus and its loops are depicted by the letters N, C and A-F, respectively. 4 transmembrane domains are labelled M1-M4, with a large intracellular loop joining the M3 and M4 domains. **Bottom left:** Diagram of the structure of the pentameric 5-HT$_3$ receptor from an extracellular view, perpendicular to the plane of the membrane (bottom left). Each large grey circle depicts a single subunit of the 5-HT$_3$ receptor, containing 4 smaller circles; the transmembrane domains M1-M4. The M2 domains are shown in white, lining the channel pore. (Thompson and Lummis, 2007)

Recently, Hassaine et al. (2014) succeeded in obtaining the crystal structure of the mouse 5-HT$_{3A}$ receptor using VHH15 molecules, termed 'nanobodies' (single chain antibodies) as crystallisation chaperones. They established the structure of the murine 5-HT$_{3A}$ receptor as 'bullet-shaped' with five subunits arranged symmetrically around a central ion channel, perpendicular to the membrane plane, as shown in figure 2.
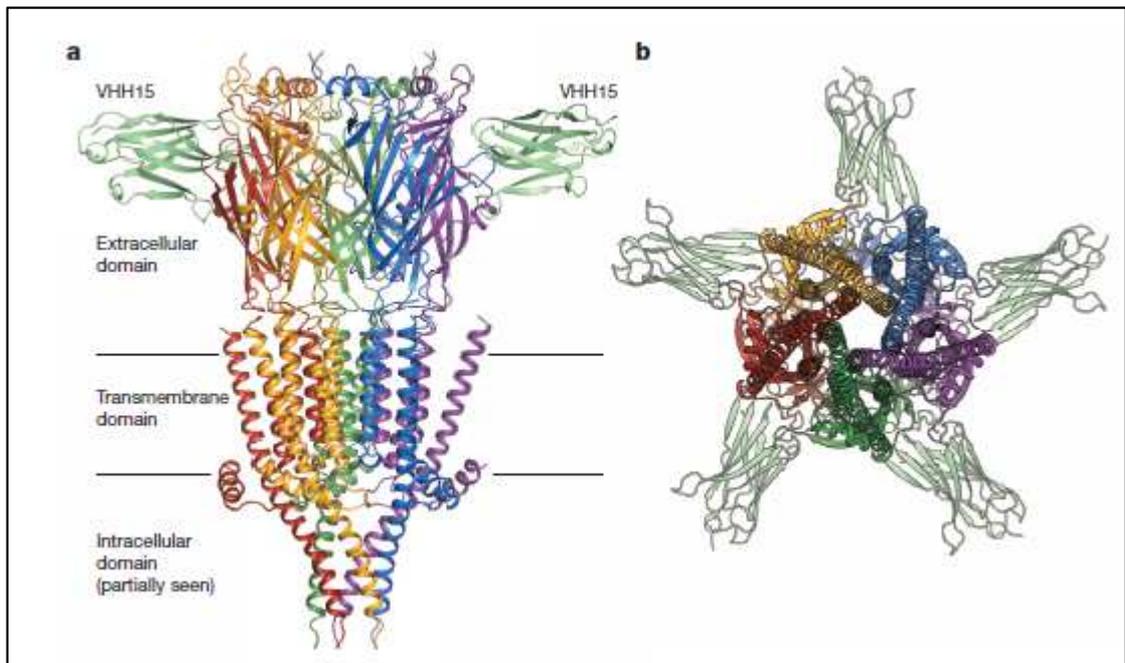
Figure 2: Crystal structure of the mouse 5-HT3 receptor in complex with VHH15 nanobodies. a: cartoon representation of the receptor parallell to the plane of the membrane. The VHH15 nanobodies are shown in light green and each subunit is represented by a different colour. b : View from above of the receptor forming the channel pore. All VHH15 molecules (light green) are visible in this plane at the interfaces between subunits. (Hassaine et al., 2014)

1.5.2.   5-HT$_{3A}$ Receptor

The 5-HT$_{3A}$ subunit was originally identified by isolation from a neuroblastoma cell line expressing high levels of the functional 5-HT$_3$ receptor (Lambert et al., 1989). The subunits assemble to form functional homopentamers in mammalian cell hosts. The HTR3A gene coding for this subunit is mapped to chromosome 11, and codes for a protein 478 to 490 amino acids in length. Distribution of the 5-HT$_{3A}$ receptor is widespread in the CNS (Kilpatrick et al., 1987), peripheral and sensory ganglia and gastrointestinal tissues (Morales et al., 1998).

1.5.3. 5-HT$_{3AB}$ Receptor

The 5-HT$_{3B}$ subunit was isolated in 1999 by screening human genomic sequence data (Davies et al., 1999). The 5-HT$_{3B}$ subunit requires co-expression with the 5-HT$_{3A}$ subunit for cell surface expression of a functional 5-HT$_{3AB}$ heteromer with distinct biophysical properties. The gene coding for the 5-HT$_{3B}$ subunit is also located on chromosome 11, and produces a 436 amino acid sequence, sharing 41% amino acid sequence identity with the 5-HT$_{3A}$ subunit (Davies et al., 1999). Atomic force microscopy by Barrera et al. (2005) revealed the heteromeric receptor contains two 5-HT$_{3A}$ and three 5-HT$_{3B}$ subunits assembled in the order B-B-A-B-A. This stoichiometry has however been widely discussed in further publications (Connolly, 2011) due to the fact that Thomson et al. (2011) revealed that A-A subunit interfaces contributed to the ligand binding site and B-B interfaces did not. Barrera et al. (2005) also included endoplasmic reticulum-retained receptors in their study, including the possibility of non-functional receptors. Other subunit orders such as B-B-B-A-A or even different stoichiometries with (3A)$_3$ and (3B)$_2$ have been suggested with the orders A-A-B-A-B or A-A-B-A-B to allow for A-A interfaces.

1.5.4. 5-HT$_{3C}$, 5-HT$_D$ & 5-HT$_E$ Receptors

The three additional 5-HT$_3$ receptor subunits are mapped on chromosome 3q27 (Niesler et al., 2008). The 5-HT$_{3C}$ and 5-HT$_{3E}$ subunits possess 36% and 39% amino acid sequence identity with the 5-HT$_{3A}$ subunit, respectively. None of the subunits, when singly expressed in a mammalian cell host, traffic to the cell surface or produce ligand binding domains and require co-expression of the 5-HT$_{3A}$ subunit for functional receptor expression at the cell surface. The heteromeric receptors do not appear to differ greatly in pharmacological profiles and their

biophysical properties are yet to be tested (Niesler et al., 2007). The 5-HT$_{3D}$ subunit has two splice variants, one lacking a large portion of the extracellular N-terminus and the other lacking a cys-cys loop (Lummis, 2012), two very important features for functional receptors. Their function is generally unknown, but hypothesised to play a role in modifying receptor function when co-expressed with other subunits.

1.5.5. The 5-HT$_3$ Receptor Ligand Binding Site

Previously, the structure and function of the 5-HT$_3$ receptor was based on homology to the nicotinic acetylcholine receptor. Strong functional and structural similarities between the 5-HT$_3$ receptor and the nACh receptor (for review, see Thompson and Lummis (2006)) were established by constructing chimeric receptors containing the N-terminus of the α7 nicotinic acetylcholine (nACh) receptor and transmembrane domains of the 5-HT$_{3A}$ receptor. These chimeras are activated by acetylcholine (ACh) and retain the channel properties of the 5-HT$_{3A}$ receptor (Eiselé et al., 1993). Furthermore, the acetylcholine binding protein (AChBP) was found to be homologous to the N-terminus of the nACh receptor. Crystallisation of the AChBP bound to nicotinic ligands brought insight into ligand recognition in the nACh receptor (Brejc et al., 2001). AChBP was also found to bind 5-HT with low affinity. Based on the homology models of the nACh receptors and mutated versions of the AChBP, Kesters et al. (2013) were able to locate the ligand binding site on the 5-HT$_3$ receptor at the interface of two adjacent subunits in the N-terminus, formed of three loops (A-C) on one principal subunit and three β-strands (loops D-F) from the adjacent (complementary) subunit. Only a few residues on the loops face the binding pocket and figure 3 below shows those contributing residues.
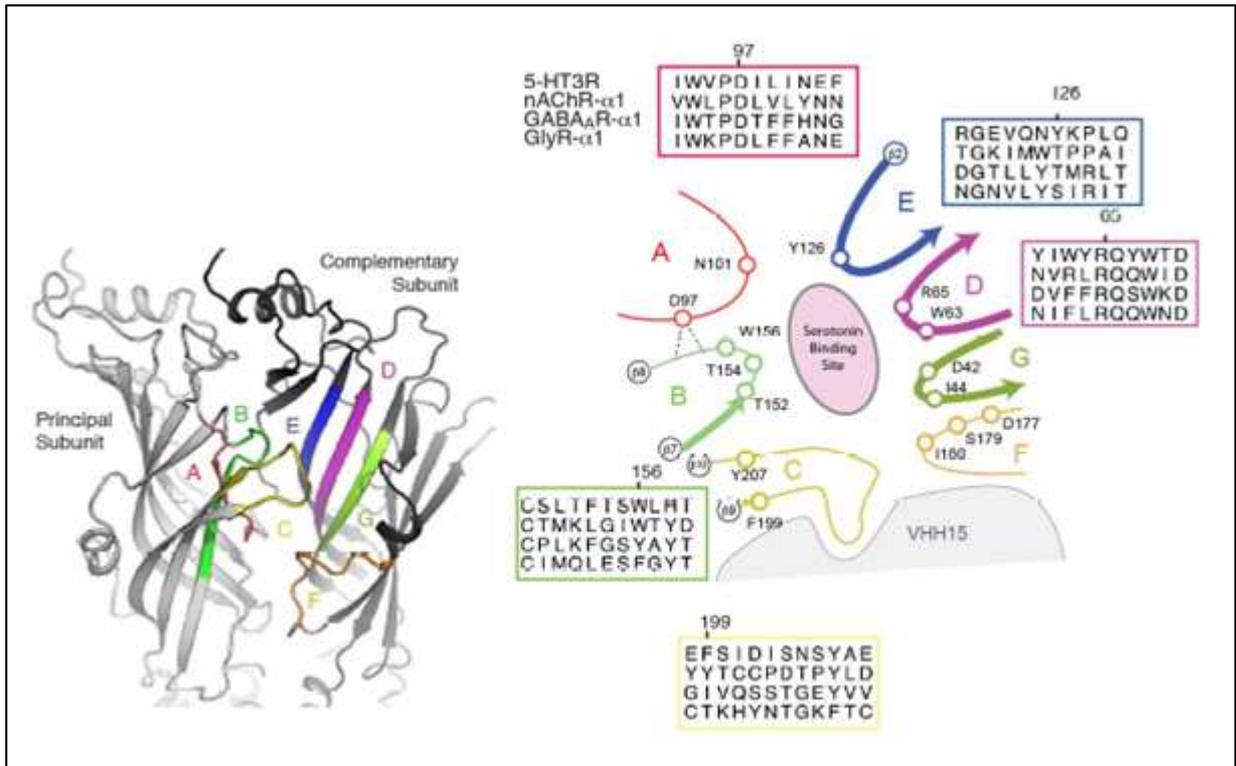
Figure 3: **Left** : Cartoon representation of the orthosteric binding site in the N-terminus, with contributing loops represented in different colours. **Right** : Diagram of the residues lining the orthosteric binding site, as well as a sequence alignment for each loop of the murine 5-HT$_3$ receptor with a human receptor of each subfamily (Hassaine et al., 2014).

X-ray crystallography revealed the orthosteric binding site was formed by the loops A, B and C from the principal subunit and portions of loops D, E and G and loop F from the complementary subunit (Figure 3, Hassaine et al. (2014)). Loops A, B, D and E appeared more internal and connected, and were thought to stabilise the structure of the ligand binding site, whereas loops C and F were more peripheral. Based on homology models of nicotinic acetylcholine receptors, it is thought loop C changes conformation to contract around 5-HT, and extends when bound to granisetron (Kesters et al., 2013).

There are also a range of potential specific binding sites for different ligands and modulators such as steroids, alcohols, anaesthetics and other small molecules (Davies, 2011).

1.5.6. Known Allosteric Modulators of the 5-HT$_3$ Receptor

There are numerous known allosteric modulators of the 5-HT$_3$ receptor. Alcohols and volatile anaesthetics such as butane are an example of positive allosteric modulators (PAMs). Compounds with small molecular volumes (such as butanol and halothane) appeared to enhance central 5-HT-evoked currents by stabilising the open state of the channel, without affecting 5-HT binding affinity (Davies, 2011). The best characterised positive allosteric modulator of the 5-HT$_3$ receptor is 5-hydroxyindole, which has been shown to display both allosteric and orthosteric effects (Kooyman et al., 1994), possibly due to its similar structure to 5-HT. Some studies showed 5-HI allosteric binding in mouse but not human 5-HT$_3$ receptors, suggesting species differences in allosteric modulation of the 5-HT$_3$ receptor (Gronlien et al., 2010). These species differences in allosteric modulation highlight the need for thorough study in human receptors. 5-HI is also a positive allosteric modulator of the α7nAChR (Zwart et al., 2002), underlining the need for a more specific research tool to study the 5-HT$_3$ allosteric binding site.

Intravenous anaesthetics such as ketamine have been shown to have non-competitive inhibitory effects on 5-HT$_3$ receptor channels at high concentrations. Propofol and barbiturates were shown to reduce 5-HT$_3$ receptor evoked currents in mouse neuroblastoma N1E-115 cells (Barann et al., 2000), suggesting non-competitive behaviour. Different categories of antidepressants (imipramine, fluoxetine and iproniazid) have all been shown to inhibit the 5-HT$_3$ receptor by blocking the receptor in the closed state (Choi et al., 2003).

Some antidepressants also accelerate desensitisation of the receptor (Fan, 1994). Other compounds shown to be allosteric modulators of the 5-HT$_3$ receptor include cannabinoids, morphine and divalent cations (Davies, 2011). These compounds show that allosteric modulation of the 5-HT$_3$ receptor is possible but their use is not relevant for targeting 5-HT$_3$ receptors in the gut, due to their non-specificity.

There are also some naturally occurring allosteric modulators of the 5-HT$_3$ receptor, including ginseng, ginger, quinine and liquorice (Davies, 2011). However, the difficulty in studying these compounds lies in the comparison of the concentrations used in vivo in traditional medicine with in vitro concentrations.

1.5.7. Ion Selection

The 5-HT$_3$ receptor is permeable to cations such as sodium (Na$^+$), potassium (K$^+$) and also calcium (Ca^{2+}). The channel pore is lined with five M2 transmembrane domains, which determine ion selectivity. Hassaine et al. (2014) demonstrated the importance of the negative charge at position D105, which is conserved in nAChRs; as well as other charged residues in the channel pore (R14, D17, K24, K25, D91, D52, D53, K54 and E186). The side chains of K108 appear to extend into the channel pore to constrict the opening. Below this constriction, rings of identical, charged amino acids in the M2 domains influence ion selection and conduction in the 5-HT$_3$ receptor (Miyazawa et al. (2003) and Hassaine et al. (2014)) . Substituting different amino acids in these rings established that single amino acids at either end of the M2 domains made the most acute difference in ion selectivity (Thompson and Lummis, 2003).

The homomeric 5-HT$_3$ receptor is equally permeable to monovalent and divalent cations. The incorporation of the 5-HT$_{3B}$ subunit appears to decrease the permeability of the 5-HT$_3$ receptor to divalent cations such as Ca^{2+} (Davies et al., 1999). The lack of an acidic residue in the outer ring of the M2 domain decreases the conductance of Ca^{2+} in nACh receptors

1.5.8.   Single Channel Conductance

The conductance of the homomeric 5-HT$_3$ receptor has been measured between 0.40 and 1 pS (Brown et al., 1998), which was found to be considerably lower than conductances measured in neuronal 5-HT$_3$ receptors. It was found that the heteromeric 5-HT$_{3A/3B}$ receptor displayed a conductance of 16 pS (Davies et al., 1999), indicating the 5-HT3B subunit plays a significant role in single channel conductance. Five portals are formed of helical amphipathic (HA) stretches located in the large intracellular loop between the M3 and M4 domains (Unwin, 2005). Substitution of the 'HA' stretch of the 5-HT$_{3B}$ subunit into the 5-HT$_{3A}$ subunit caused an increase in conductance similar to that of the heteromeric 5-HT$_{3A}$ receptor (Kelley et al., 2003), associating the cytoplasmic region with determining single channel conductance.

1.6.   Irritable Bowel Syndrome

Irritable bowel syndrome affects approximately 5-10% of the global population (Spiller, 2011). There are no biomarkers of IBS, rather the disease is characterised by recurrent symptoms of abdominal pain or discomfort associated with irregular bowel habits, based on the Rome III Diagnostic Criteria for Functional Gastrointestinal Disorders (2006). The diagnostic criterion for irritable bowel syndrome is recurring abdominal pain or discomfort

for at least three days per month in the last three months associated with at least two symptoms regarding bowel habits.

IBS is sub-classed into three categories depending on the predominant bowel symptom: diarrhoea-predominant (IBS-D), constipation-predominant (IBS-C) or IBS alternating diarrhoea and constipation, termed mixed (IBS-M). Symptoms can manifest between the ages of 15 and 65, and are more prevalent in women. Although not lethal, IBS can cause severe reduction in quality of life and lead to significant healthcare costs due to symptoms and IBS-associated diseases, loss of productivity and work absenteeism. In the USA, IBS costs society between $1.7 and $10 billion annually (Hulisz, 2004), justifying research into better treatment of symptoms.

1.6.1.   The Role of the 5-HT$_3$ Receptor in Irritable Bowel Syndrome

The vast majority (90-95%) of 5-HT in the body is located in the gastrointestinal system and it plays an important role in normal gut function. It interacts with the enteric nervous system (ENS); a complex network of approximately 100 million neurons. The majority of 5-HT in the gut is stored in enterochromaffin cells forming the lining of the GI tract, which function as sensory transducers by releasing 5-HT in response to luminal stimuli such as pressure or nutrients (Spiller, 2011). A small amount of 5-HT is also found in neurons in the myenteric plexus of the ENS. 5-HT activates intrinsic and extrinsic primary afferent neurons to stimulate peristalsic and secretory functions, respectively, and relay sensory information to the central nervous system (Gershon and Tack, 2007). Figure 4 below illustrates the pathways stimulated by 5-HT release in the gut. 5-HT$_3$ receptors have been shown to mediate intestinal secretion (Hansen and Skadhauge, 1997), neurogenic smooth muscle contractions in the guinea pig

ileum (Buchheit et al., 1985) and increased colonic motility (Talley et al., 1990). These symptoms have been blocked by 5-HT$_3$ receptor antagonists such as ondansetron, alosetron and ramosetron, reinforcing the notion of 5-HT$_3$ receptor implication in IBS-D (Spiller, 2011).
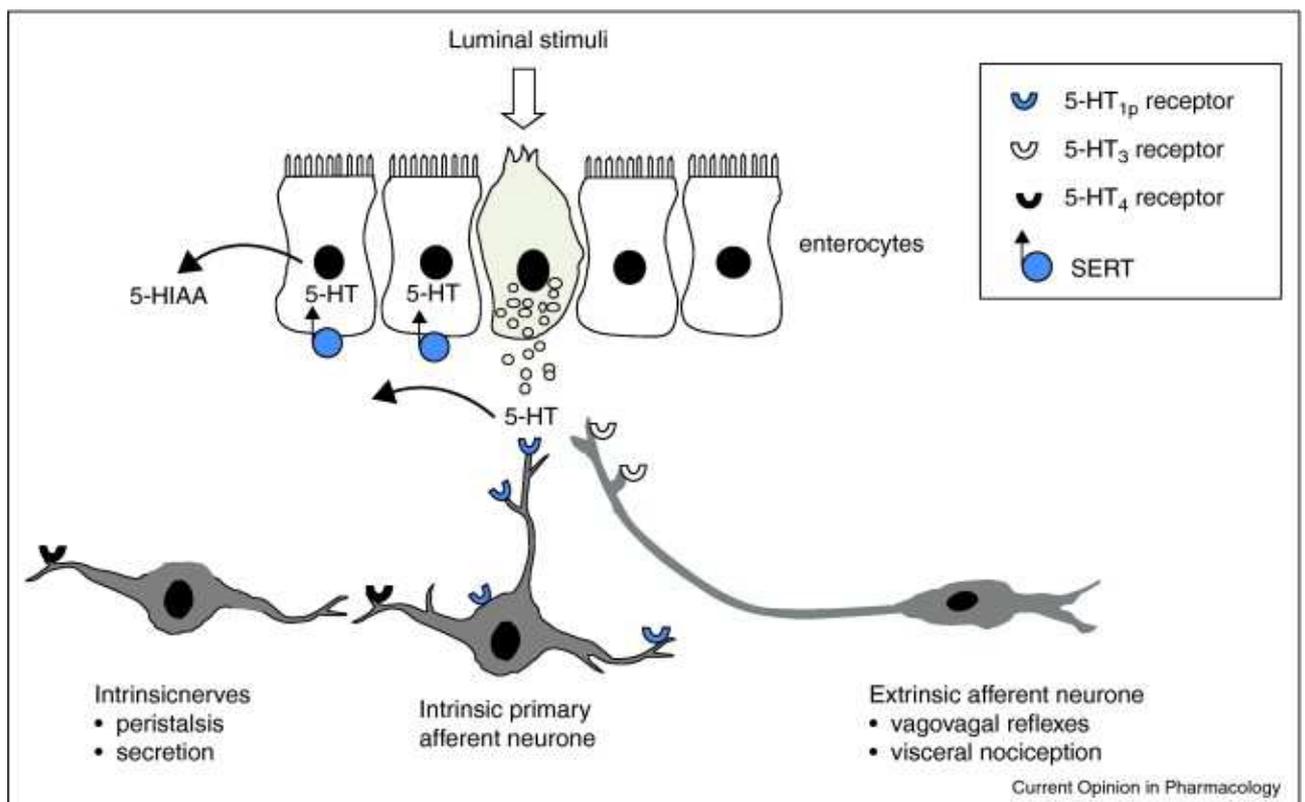
Figure 4: Illustration of the 5-HT receptors involved in the physiological and pathophysiological responses to mucosal stimuli. 5-HT is stored in enterochromaffin cells (in white) and released in response to luminal stimuli. 5-HT binds to a variety of nerve endings in the enteric nervous system. 5-HT1p receptors (poorly characterised receptors found in the ENS) are found on intrinsic primary afferent neurons (IPANs), 5-HT$_3$ receptors are located on extrinsic afferent neurons (vagal and splanchnic nerves) and on myenteric nerves (not shown) and 5-HT$_4$ receptors are found throughout the myenteric plexus. Signalling is terminated by reuptake via the serotonin transporter (SERT, in blue) into the enterchromaffin cells, where 5-HT is metabolised by monoamine oxidase to 5-hydroxyindole acetic acid (5-HIAA). (Spiller, 2011)

1.6.2. Use of 5-HT$_3$ Receptor Antagonists to Treat IBS-D

Ondansetron was the first 5-HT$_3$ receptor antagonist to be successfully used to treat the symptoms of IBS-D, however, the more potent alosetron was selected for clinical trials as it was 3-10 times more potent with longer lasting alleviation of symptoms (Spiller, 2011). A meta-analysis of 14 randomised controlled trials (RCT) (Andresen et al., 2008) showed administration of alosetron and cilansetron (compared to placebo and mebeverine, an antimuscarinic antispasmodic used to treat IBS) significantly alleviated symptoms of IBS and were more effective than the comparators. A common side effect of using 5-HT$_3$ receptor antagonists was constipation (Andresen et al., 2008), which was cause for approximately 10% of patients reporting constipation to discontinue treatment.

1.6.3. Ischaemic Colitis

Alosetron was approved by the Food and Drug Administration (FDA) in February 2000 and marketed by Glaxo Wellcome as Lotronex, but within a few months received 70 reports of complications, including 49 of ischaemic colitis and 21 of severe constipation with ruptured bowels. Of those 70 cases, 34 were hospitalised, 10 required surgery and 3 deaths were reported (Lisi, 2002). As a result of further reports of adverse effects, Glaxo Wellcome voluntarily withdrew alosetron in 2000, but reintroduced it in 2002 with a more restricted indication and prescribing program to treat only women with severe diarrhoea-predominant IBS (FDA, 2012).

A review of 29 072 patients administered with alosetron under a risk management plan showed the incidence of complications around 0.95 cases per 1000 patient years and the

symptoms abated when treatment was discontinued (Chang et al., 2010). There were no reported surgeries required or any deaths reported, as was previously shown in 2000. Ramosetron, another 5-HT$_3$ receptor antagonist is still currently used to treat IBS-D in Japan (Matsueda et al., 2008).

It seems the rationale behind prescribing 5-HT$_3$ antagonists is sound but the restricted access for patients limits the beneficial effects. This justifies the need for efficient drugs targeting the 5-HT$_3$ receptor but without the severe side effects of prolonged antagonism. An interesting observation is that 5-HT$_3$ receptor antagonists are widely prescribed to treat chemotherapy-induced nausea and vomiting post-surgically, yet ischaemic colitis has not been reported as a side effect when used in this context. This suggests there could be interactions of 5-HT$_3$ receptor antagonists specific to patients with IBS.

1.7.   Allosteric Modulation

The success of 5-HT$_3$ receptor antagonists such as alosetron to treat the symptoms of IBS-D but their failure in their side effect profile emphasises the requirement for a functionally similar compound which does not fully block 5-HT$_3$ receptor activity. This is the rationale behind allosteric modulators. This would enable a compound to either increase (positive allosteric modulator PAM) or decrease (negative allosteric modulator NAM) the activity of a receptor in response to the endogenous ligand whilst binding to a different site. These compounds have no effect on receptor activity alone, but function by potentiating or reducing the response to an agonist or partial agonist.

It is hypothesised that a negative allosteric modulator (NAM) would alleviate the 5-HT_3 receptor-mediated symptoms such as nociception, excessive secretion and peristalsis without fully abolishing basal levels for normal bowel function.

1.7.1. 5-Chloroindole

5-Chloroindole (5-Cl) has recently been identified as a potent and selective allosteric modulator of the 5-HT_3 receptor (Newman et al., 2013). It was shown to potentiate 5-HT_3 receptor agonist and partial agonist responses by increasing the affinity of these agonists for the receptor and by reactivating desensitised 5-HT_3 receptors both in cell lines expressing the recombinant receptor and native tissues (Newman et al., 2013). This study also showed that potentiation of agonist-evoked responses did not occur in α7 nicotinic acetylcholine receptors. Unpublished data (Grafton G., personal communication) have also found that 5-chloroindole had no potentiating effect on 5-HT-evoked responses in a (rat/mouse) chimeric $α7_{V201}5\text{-HT}_3$ receptor (first described in Eiselé et al. (1993)). This chimeric receptor possesses the N-terminus of the α7 nicotinic acetylcholine receptor, suggesting the binding site for 5-Cl is in the N-terminus of the 5-HT_3 receptor.
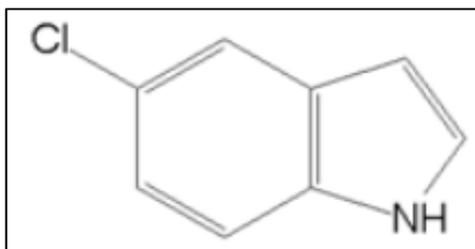
Figure 5: Diagram of the chemical structure of 5-chloroindole. Taken from Sigma Aldrich

1.8.   Aims

Although it has no likely use clinically due to projected pro-emetic and anxiogenic effects, 5-chloroindole has proven to be a useful tool for characterising the nature and structure of the allosteric binding site. In this present dissertation, I have investigated derivatives of 5-Cl to determine a core structure which will bind with high affinity to the allosteric binding site, and understand the molecular determinants of negative allosteric modulation. I have also attempted to construct a human/human $\alpha 7_{V201}$5-HT$_3$ chimeric receptor to confirm findings in the equivalent rat/mouse chimera, and locate the allosteric binding site to the N-terminus of the 5-HT$_3$ receptor. Expanding our knowledge of the structure-activity relationship of the allosteric binding site will allow a more rational drug design of negative allosteric modulators with potential therapeutic benefits.

CHAPTER 2 : MATERIALS AND METHODS

2.1. Use of Mammalian Cell Lines

2.1.1. Maintenance of HEK-293 Cells

Stable cell lines expressing recombinant human $5\text{-}HT_{3A}$ receptors were cultured in complete medium containing Dulbecco's Modified Eagle's Medium (DMEM, Sigma, D5796) supplemented with 10% (v/v) foetal bovine serum (FBS, Sigma F2442) and a 100 µg/mL penicillin/streptomycin antibiotic solution (Invitrogen, 15140122). The cells were grown in 75cm^2 (T75) sterile tissue culture flasks in a LEEC cell culture incubator which maintains 100% relative humidity, the temperature at 37°C and the CO_2 levels at 5%. Sterile conditions were maintained by using a class II microbiological safety cabinet (air filtration system), using filter sterilised solutions (Millipore 0.22 µM filters), sterile serological pipettes and autoclaved utensils.

Cells were regularly passaged to maintain healthy proliferation and provide room for growth. Around 100% confluence, the medium was aspirated off the cells, which were then washed with Ca^{2+}- and Mg^{2+}-free phosphate buffer saline (PBS, Invitrogen, 14200067) and incubated for 5 minutes at 37°C in a 1 mL trypsin/EDTA solution (2.5 g/L and 0.2 g/L respectively, Sigma, T4174). Once trypsinised, complete medium was added to the cells to inhibit the trypsin. Routinely, 9 mL medium was added to the flask, to makeup a final volume of 10 mL. To perform a 1:5 passage, 2 mL were taken from this 10 mL cell suspension and transferred to a new flask, and the final volume made up to 15 mL with medium. The factor of dilution refers to the volume of cells taken from the diluted trypsin cell suspension, and manipulating this dilution factor controls the speed of growth and proliferation. Human embryonic kidney

293 (HEK293) cells transfected with DNA encoding the 5-HT$_{3A}$ receptor required weekly innoculations with 0.5 mg/mL geneticin (G418). The number of passages was recorded by adding 1 to each generation number and cells were considered viable up to passage 45.

2.1.2. Preparation of Whole Cell Lysates

Protein samples for experiments were obtained from cell lines expressing the protein of interest. Once the medium was removed and the cells washed with 5 mL PBS, the cells were removed using a cell scraper, which physically scrapes the cells off the bottom of the flask. The cells were then resuspended in 10 mL PBS and transferred to a 50 mL centrifuge tube, and centrifuged at 400 x g for 5 minutes. The supernatant PBS was aspirated and discarded to leave a cell pellet at the bottom of the tube. Cell pellets being used for downstream experiments were resuspended in 1 mL 50 mM Tris pH7.4 and kept on ice. Those not being used immediately were stored dry at -80°C for later use.

To obtain whole cell lysates, the cells were homogenised to release intracellular proteins and liberate cell surface proteins. Cells were lysed using a sonicator, a vibrating probe which vibrates at a high frequency to disrupt cell membranes. The samples were sonicated on ice in 5 pulses of approximately 5 seconds each, so as not to overheat the protein.

2.1.3. Bradford Protein Quantitation

The Bradford protein assay is a colourimetric protein assay. The colour change is caused by binding of protein to Coomassie Brilliant Blue G-250. The increase of absorbance at 595 nm

is proportional to the amount of bound dye, and thus to the amount (concentration) of protein present in the sample. The Bradford assay is linear at a range of 100 to 1400 µg/mL (for the reagent used).

The spectrophotometer was calibrated using bovine serum albumin, the most widely recognised protein standard for Bradford protein assays. 20 µL of concentrations of bovine serum albumin (BSA) ranging from 0.2 to 1 mg/mL were added to 1 mL Bradford reagent (Sigma, B6916).

The spectrophotomer was initially blanked with 1 mL Bradford reagent and 20 µL of 50 mM Tris pH 7.4, then 20 µL of the samples were incubated in 1 mL Bradford reagent at room temperature for at least 5 minutes to allow the colour to develop. The spectrophotometer would display both the absorbance of the sample and the sample protein concentration, obtained from calibration. The whole cell homogenates could then be diluted in 50 mM Tris pH 7.4 to the desired concentration for further experimentation.

2.2.   Assessment of $[Ca^{2+}]_i$

FlexStation analyses measure the amounts of free cytoplasmic calcium in HEK293 cells expressing human $5\text{-}HT_{3A}$ receptors. The calcium-binding dye Fluo-4 AM (acetoxymethyl) is a lipid-soluble ester which permeates the cell membrane. Once inside the cell, the host cell esterases cleave the AM compound, rendering fluo-4 trapped inside the cell, thus enabling the intracellular calcium to be labelled. Activation of the $5\text{-}HT_{3A}$ receptor will thus trigger the influx of Ca^{2+} ions, causing an increase in fluorescence once the dye has bound to calcium. One pitfall of this method is that the limiting factor is the amount of fluo-4 inside the cell,

signifying the response is saturatable. Other calcium binding dyes were also tested, but showed no difference in saturation levels (data not shown).

Black-walled, clear bottom, 96-well plates (Corning, CLS3603) were treated with sterile, warm, poly-D-lysine (Sigma, P6407) for 30 minutes in a biological safety hood. The poly-D-lysine was then removed and the remnants were rinsed off with filter sterilised water. Once dry, the plates were ready to be used for tissue culture.

HEK293 cells expressing human 5-HT_{3A} receptors were plated at approximately 1×10^5 cells per well and incubated overnight in DMEM in a tissue culture incubator. In preparation for FlexStation analysis, the cells were rinsed twice in Hank's balanced salt solution (HBSS) buffer (Gibco, 14025092) and then incubated with 5 µM Fluo-4 AM (Invitrogen, F-14201) for one hour at room temperature. The cells were then washed twice in HBSS and then incubated in HBSS for a further 30 minutes to remove any extracellular fluo-4.

Drug plates (96-well clear-walled, clear bottom, Corning, 2503) were prepared with ranging concentrations of the drugs of interest. The drugs plate and cell plate were loaded into and run by a FlexStation benchtop scanning fluometer (Molecular Devices), which reads the column of 8 wells simultaneously, over a time course, during which up to three compounds can be added. Alterations of intracellular calcium concentrations in response to various concentrations of 5-HT (10^{-5} to 10^{-8}) in the absence and presence of various compounds were measured.

2.3. Radioligand binding

Competition radioligand binding studies the ability (or lack of) of a 'cold' unlabelled compound to compete at different concentrations for a specific target with one concentration of a radiolabelled compound ('radioligand'). The amount of radioligand still bound to the target can then be measured by liquid scintillation counting, and a binding curve produced. All data are produced in triplicates.

Ice cold 50 mM Tris buffer (Trizma base, Sigma), pH 7.4, was used throughout the experiment for dilution of drugs, cell membrane preparations and the washing stage during harvesting. 'Cold' competing drugs were weighed and diluted in buffer or initially to stock concentrations of 10 mM, then diluted to concentrations spanning their IC_{50}s, the concentration of drug producing 50% of a response. Allosteric modulators were diluted in dimethyl sulphoxide (DMSO, Sigma, D8418), due to their insolubility in water.

Drug	Manufacturer, Product number	Molecular Weight (g/mol)	Dissolved in
Radioligand			
[3H]-granisetron: BRL-43694, [9-methyl-3H]	Perkin Elmer, NET1030250UC	1 µCi/µL in 100% ethanol	50 mM Tris
Cold Competing Drug			
5-HT	Sigma, H9523	292.93	50 mM Tris

Ondansetron	Tocris Bioscience, 2891	329.83	50 mM Tris
Quipazine	Sigma, Q1004	329.40	50 mM Tris
(S)-zacopride	Department of Chemistry, University of Birmingham	345.20	50 mM Tris
Allosteric Modulators			
5-Chloroindole	Sigma, C47604	151.59	DMSO
5-(trifluoromethyl)-indole	Sigma, 701068	185.15	DMSO
5-bromoindazole	Department of Chemistry, University of Birmingham	151.70	DMSO
5-bromo-benzimidazole	Department of Chemistry, University of Birmingham	151.50	DMSO

The buffer, allosteric modulators, 'cold' drug, radioligand and membrane preparations were added in triplicates to binding tubes to a final volume of 500 µL as shown in table 1. Concentrations of the 'cold' drugs were prepared 3 x concentrated and the radioligand was prepared 5 x concentrated so as to reach the correct final concentration in the total reaction volume. The samples were incubated at room temperature for one hour before termination by rapid filtration. During this incubation time, glass fibre filters (Whatman GF/B, Brandel) were soaked in a 0.3% polyethyleneimine solution (PEI, Sigma, P3143).

	Buffer (µL)	'Cold' drug (µL)	Radioligand (µL)	Membranes (µL)
Control	150	0	100	200
Experimental conditions	0	150	100	200

Table 1: Volumes of reagents added to binding tubes. Control tubes are to show total binding. Experimental conditions describe the range of concentrations of competing drug added.

A 48 sample Brandel cell harvester was used to terminate the reactions by separating unbound ligand from ligand-bound receptor through the glass fibre filters. The system, joined to a vacuum pump aspirates the samples in the tubes, whilst washing with ice-cold 50 mM Tris pH 7.4. Samples were washed 3 times for 4 seconds each.

Once samples were harvested, the filtration unit was opened, the filters were cut and placed into polypropylene scintillation vials, and soaked overnight in 4 mL of scintillation cocktail (Scintisafe 3, Fisher). The next day the scintillation vials were placed in a Packard 1500TR Liquid Scintillation Analyser to measure the amount of radioligand-bound receptor on the filters in disintegrations per minute (DPM).

2.4. Data Interpretation

In intracellular calcium (FlexStation) studies, data (relative fluorescent units RFU) were analysed in SoftMax Pro 4.8 and RFU was plotted as a percentage of the maximal 5-HT response in Kaleidagraph 3.5 (Synergy).

In radioligand binding studies, data were plotted as DPM against the concentration of competing drug in KaleidaGraph 3.5, (Synergy), and a four parameter logistical equation was used to obtain the IC_{50} and Hill number for each curve.

Below is the logistical equation used:

$$m4-(m1*((m0\wedge m3)/((m0\wedge m3)+(m2\wedge m3))))$$

Where: **m1** is the specific binding (total – non-specific binding)

              m2 is the IC_{50} of the drug

              m3 is the Hill coefficient

              m4 is the total binding

The total binding (m4) and specific binding (m1) were corrected by inserting values obtained from initial curve fits.

The Ki of the drug was calculated using the Cheng-Prussoff equation:

$$Ki = \frac{IC_{50}}{(1+\frac{[RL]}{Kd})}$$

Where : IC_{50} of the 'cold' drug

              [RL]: concentration of radioligand

              Kd: dissociation constant of the radioligand

2.5.   Statistical Analysis

Data obtained from graphical analysis were analysed using GraphPad Prism 5.0. The Kd (dissociation constants) and Hill coefficients obtained from radioligand binding competition studies were initially tested for normality using the Shapiro-Wilk normality test. As the data were found to not be normally distributed, the Mann-Whitney U test was adopted.

Analysis of variance (ANOVA) was used to compare data points and test for a significant difference between any data points on graphs. Significance was reached if $p < 0.05$.

2.6.   Methods in DNA Preparation

2.6.1. Plasmid Vectors

2.6.1.1. α7 Nicotinic Acetylcholine Receptor

The human α7 nicotinic acetylcholine receptor nucleotide sequence (GenBank accession no. NM_000746.5) was inserted into pCI-neo (Promega, E1841), a 5.5kb plasmid with a cytomegalovirus (CMV) enhancer/promoter region; with NotI/XhoI ends. It contains a bacterial resistance gene for ampicillin, and a neomycin phosphotransferase gene, which acts as a selectable marker for mammalian cells. Below is the map of pCI-neo with the insert, constructed in Serial Cloner v 2.6.1.
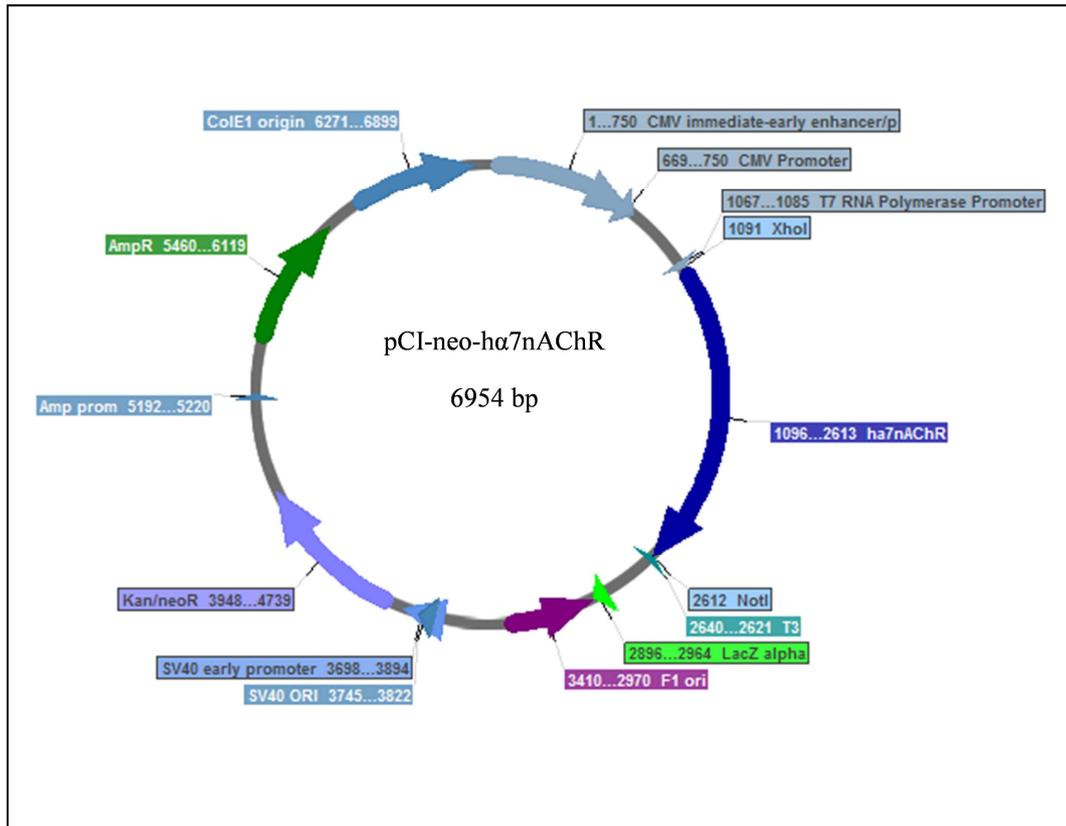
Figure 6: Plasmid map of the pCI-neo vector with human α7 nicotinic acetylcholine receptor insert. Reference points and positions in the plasmid are indicated in the map (obtained from Promega) : F1 ori : F1 origin, Kan/neoR : kanamycin /neomycin resistance gene, AmpR : ampicillin resistance gene.

2.6.1.2. 5-HT$_{3A}$ Receptor

The human 5-HT$_{3A}$ receptor nucleotide sequence (GenBank accession no. NM_000869.5) was inserted into pcDNA3.1/myc-His (Invitrogen, V800-20), a 5.5kb plasmid, also expressing a CMV enhancer/promoter region; with BamHI/XbaI ends. It contains a bacterial ampicillin resistance gene, and a neomycin phosphotransferase gene for transfected cell selection. Below is the map of the pcDNA3.1 with the human 5-HT$_{3A}$ insert.
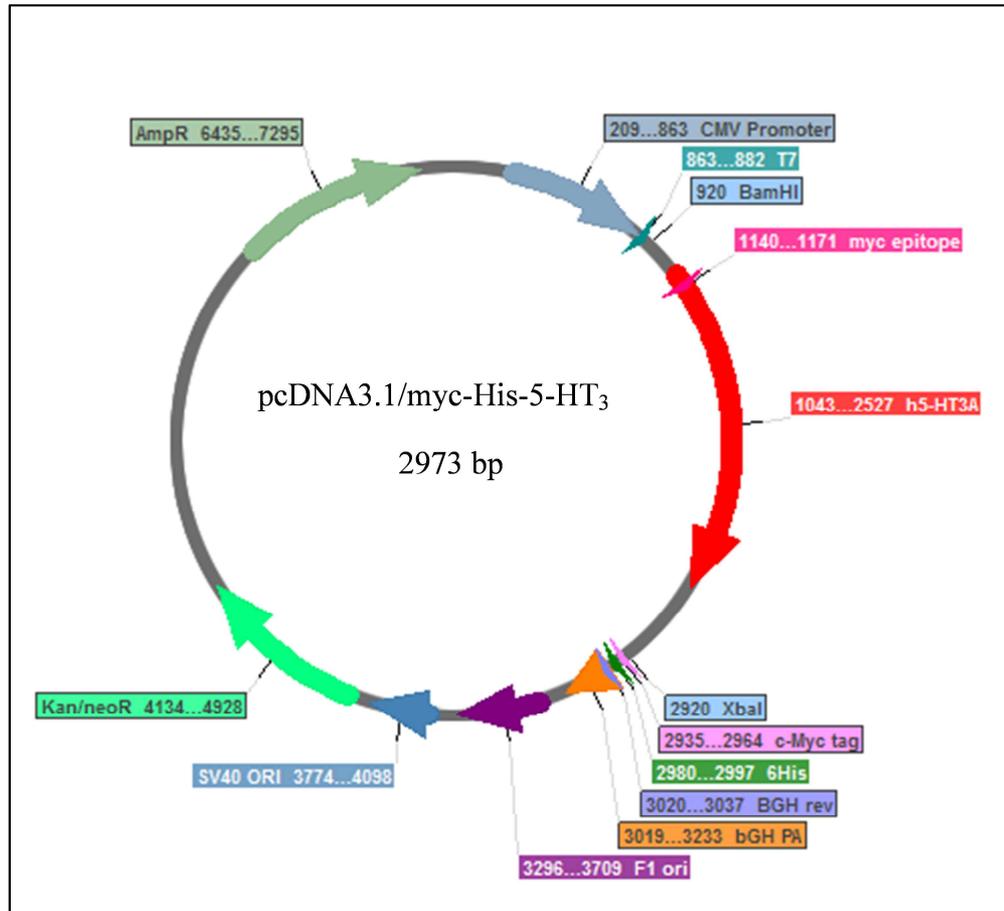
Figure 7: Plasmid map of pcDNA3.1/myc-His with human 5-HT$_{3A}$ insert. Reference points and positions in the plasmid are indicated in the map (obtained from Invitrogen). T7 : T7 promoter, h5-HT3A : human 5-HT$_{3A}$ insert, 6His : his tag, BGH rev : BGH reverse plasmid primer, bGH PA : bGH PA terminator, F1 ori : F1 origin, SV40 ori : SV40 origin, Kan/neoR : Kanamycin / neomycin resistance gene, AmpR : ampicillin resistance.

2.6.2. DNA Sequencing

Native and recombinant plasmid DNA was sequenced by dye-termination sequencing, derived from Sanger's chain-termination method (Sanger and Coulson, 1975), by the Functional Genomics Facility (University of Birmingham). Sequences were imported and chromatograms visualised using Chromas Lite v2.1.1. Chromatograms appear as the DNA sequence with peaks of colour representing each nucleotide (thymine in red, adenine in green,

35

guanine in black and cytosine in blue). The height of a peak represents the degree of fluorescence for a nucleotide in that position; hence the higher the peak, the higher the fluorescence. Additionally, above each peak is a coloured bar, representing the order of magnitude of the probability of error for that base. A full bar indicated a probability of less than 1:1 000 000 that the base is incorrect. The quality of the chromatogram can thus be determined by these indicators, and viable sequences were selected on this basis. The sequence files were then exported to a FASTA format to analyse the data. The FASTA files were copied into BLAST and aligned with the consensus sequences for each receptor (See sections 2.6.1.1. and 2.6.1.2.)

2.6.3. DNA Quantitation

DNA obtained from PCR or gel extractions was purified and resuspended in nuclease-free water. The DNA concentration in solution was measured using a microvolume spectrophotometer (Nanodrop 2000™, Thermo Scientific).

The Nanodrop was initially blanked by pipetting 2 µL of the nuclease-free water in which the DNA was resuspended. DNA was measured (in ng/µL) by adding 2 µL of the DNA sample to the Nanodrop. DNA is measured at 260 nm, the wavelength at which it absorbs light (Dahm, 2008)., the sample is exposed at 280nm to measure for sample purity and the ratio of absorbances at 260 and 280nm (260/280) is calculated. A ratio of 1.8 is generally accepted as pure for DNA. If the ration is lower, this could indicate the presence of proteins or other contaminants that absorb strongly at 280nm. A secondary measure of sample purity is the 260/230 ratio. Pure sample ratio values are expected around 2-2.2.

2.6.4. Agarose Gel Electrophoresis

Agarose gel electrophoresis was used to separate DNA fragments by size. A 1% agarose gel was made with 2 g agarose in 200 mL 1 X TAE buffer (see table 3) and heated to dissolve the agarose powder. Once cooled, 20 µL Sybr®Safe was mixed into the gel, which was then was cast in a casting tray with sealed edges and a comb, and left to set. The gel was placed in an electrophoresis tank (Thistle Scientific) and submerged in 1 X TAE buffer.

50X TAE Buffer – 1L	
Trizma Base (Sigma T1503)	242g
Glacial Acetic Acid (Fisher 10304980)	57.1mL
EDTA (0.5M)	100mL

Table 2: Composition of 50 X TAE Electrophoresis Buffer

1% Agarose Gel	
1X TAE buffer	200 mL
Agarose (Sigma A9539)	2 g
Sybr®Safe DNA Gel Stain (Invitrogen S3312)	20 µL

Table 3: Composition of 1% Agarose Gel

To allow identification of samples, 5 µL HyperLadder™ I (Bioline, BIO-33053) was loaded directly into one well. 5 X DNA loading buffer (Bioline, BIO-37045) was added to DNA samples to a final 1 X concentration, then samples were loaded into wells in the gel. The gel was typically run at 100 V for between 1 and 1.5 hours, depending on fragment size.

Once the gel had run, it was removed from the electrophoresis tank and placed in a gel visualiser (Syngene) coupled to a computer to adjust lighting settings and take screen shots of the gel. The bands obtained could be compared to the DNA ladder to determine their size. The gel could then be placed on a blue light transilluminator (Invitrogen), and the desired bands were cut out using a scalpel blade for downstream molecular biology.

2.6.5. Gel Extraction and Purification

DNA bands of interest were excised from the agarose gel and the DNA extracted from the gel using a commercially available kit (GenElute Gel Extraction Kit, Sigma, NA1111), following the manufacturer's specifications. The kit combines silica binding technology with a spin

column format to separate the DNA from the agarose gel. The gel slices were weighed, then three gel volumes of gel solubilisation solution added (i.e. for 100 mg of gel, 300 µL of gel solubilisation solution was added). The gel slices were incubated in a water bath at 60°C for 10 minutes, allowing the gel to melt. One gel volume of 100% isopropanol was added to precipitate the DNA. The solution was then loaded into columns containing a silica membrane and spun in a microcentrifuge at 12 000 x g for 1 minute, and the flowthrough was discarded. The column was then washed with wash solution containing 100% ethanol, to wash salts and impurities out of the matrix. The DNA was finally eluted out of the silica membrane and collected in a microcentrifuge tube by using 50 µL of low ionic elution buffer.

To resuspend the DNA in nuclease-free water and remove impurities caused by the extraction process, the DNA was purified using the purification steps described in step 2.6.6.

2.6.6. DNA Purification

DNA samples were incubated at -20°C for 20 minutes with 0.1 volumes of 3 M sodium acetate pH 5.2 (Sigma, 71196) and 2.5 volumes of ice cold 100% ethanol, to precipitate the DNA. They were then spun in the microcentrifuge at 14 000 x g for 30 minutes to pellet the DNA. The supernatant was removed, and then samples were spun again for 1 minute in 1 mL 70% ice cold ethanol. Two washes in 1 mL 100% ice-cold isopropanol were then performed in the microcentrifuge at 14 000 x g for 1 minute each. The samples were then left to air dry, and resuspended in 100-500 µL nuclease-free water.

2.6.7.   Construction of a Chimeric α7$_{V201}$5-HT$_{3A}$ Receptor

2.6.7.1. Overlap Extension Polymerase Chain Reaction

Overlap extension PCR is a form of PCR allowing two fragments of DNA to be amplified and joined together. This method was used with the aim of constructing the chimeric α7$_{V201}$5HT$_{3A}$ receptor.

Primers in table 4 were designed using the online nucleotide and protein sequence storing tool Biology Workbench (San Diego Supercomputer Center), then synthesised by Alta Bioscience Ltd (University of Birmingham) and Sigma. The primers were resuspended in nuclease-free water to a stock concentration of 100 µM, according to the manufacturer's specifications; then diluted in nuclease-free water to the correct concentrations for downstream use.

The forward flanking (FF) primer sequence was complementary to the 5' end of the α7 nicotinic acetylcholine receptor N-terminus, and the reverse chimeric primer (RC) was complementary to the 3' end of the N-terminus sequence (in blue), and the 5'end of the 5-HT$_{3A}$ receptor (in red). These two primers were used to amplify the α7nACh N-terminus sequence. The reverse flanking primer (RF) was complementary to the 3' end of the 5-HT$_{3A}$ receptor sequence, and the forward chimeric primer (FC) was complementary to the 3' end of the α7nACh N-terminus sequence and the 5' end of the 5-HT$_{3A}$ template. These two primers were used to amplify the 5-HT$_{3A}$ sequence.

Primer Name	Primer Sequence
α7 Forward Flanker FF (Alta Bioscience)	5'-TCACTATAGGGATCCCTCGAGGCCACCATGCGCT-3'
α7/3A Reverse Chimeric RC (Sigma)	5'-CCGCCGGCGGATGACCACTGTGAAGGTGACAT-3'
α7/3A Forward Chimeric FC (Sigma)	5'-ATGTCACCTTCACAGTGGTCATCCGCCGGCGG-3'
3A Reverse Flanker RF (Alta Bioscience)	5'-GTTCGAAGGGCCCTCTAGATGCATGCTCGAGGTCG-3'
Chimeric Reverse Primer CRev1 (Sigma)	5'- GGCCGCCGGCGGATGACCACTGT - 3'

Table 4: Primer name and sequence used for overlap extension PCR. Blue sequences represent α7 nAChR sequences. Red sequences represent 5-HT$_{3A}$ sequences. Green sequences show restriction sites BamHI in the α7 FF primer, XbaI in the 3A RF primer and MreI in the CRev1 primer.

In the first step of overlap extension PCR, a 50 µL PCR preparation consisted of: 5µL of 10X Pfu Polymerase buffer with MgSO$_4$ (Promega, M776A), 100 ng of each DNA template, 25-50 µmoles of one flanking primer and one chimeric primer, 200 µmoles of each deoxynucleotide triphosphate (dNTPs, Promega U1515), 1.5-3 units Pfu Polymerase (Promega M774A) and the final volume completed to 50 µL with nuclease-free water.

The PCR was conducted in the conditions as described in tables 5 and 6. The products obtained were one α7nACh receptor N-terminus sequence with a 3' overhang belonging to the 5-HT$_{3A}$ receptor sequence, and one 5-HT$_{3A}$ fragment with a 5' overhang belonging to the α7nACh receptor sequence. The 5-HT$_{3A}$ overhang on the α7nACh receptor fragment is

complementary to the 5'end of the 5-HT$_{3A}$ fragment, and the α7nACh overhang on the 5-HT$_{3A}$ fragment is complementary to the 3' end of the α7nACh fragment. The PCR products were separated by agarose gel electrophoresis to identify the correct bands (see section 2.6.4). The bands of the correct size (721 bp for the α7nAChR fragment and 1.1 kb for the 5-HT$_{3A}$ fragment) were extracted and purified from the gel. The PCR products obtained possessed complementary overhangs, therefore were introduced in a second round of PCR with only the FF and RF primers to produce the full chimeric sequence.
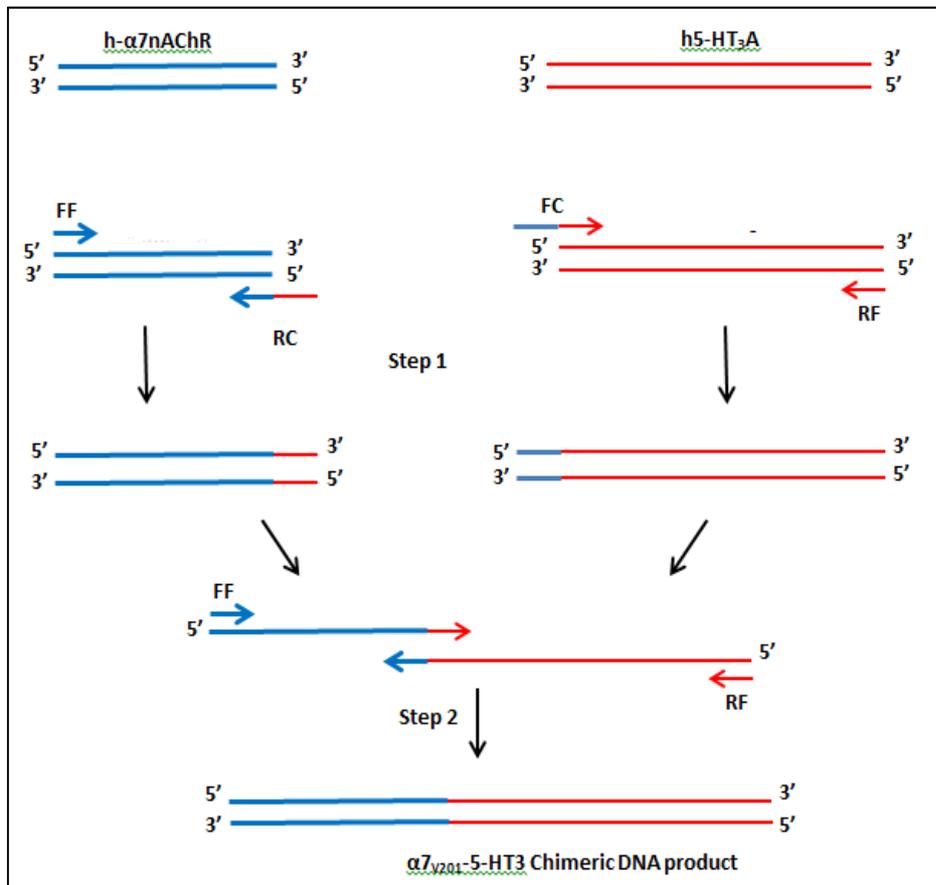
Figure 8: Graphical representation of overlap extension PCR of the human nicotinic acetylcholine receptor (h-α7nAChR, blue) sequence and human 5-HT$_{3A}$ receptor (h5-HT$_{3A}$, red) sequence to form a chimeric human/human α7$_{V201}$5-HT3 receptor sequence. Arrows represent complementary primers. FF: forward flanking primer, RF: reverse flanking primer, FC: forward chimeric primer, RC: reverse chimeric primer.

PCR reaction	
10 X Pfu Buffer Promega M776A	5 µL
DNA Template	100 ng
Complementary primers	25-50 µmoles
dNTPs Promega U1515	200 µmoles each
Pfu polymerase (units U) Promega M774A	1.5-3 U
ddH$_2$O	Make up to 50 µL

Table 5: PCR reaction components

Step	Temperature (°C)	Time (minutes)	Cycles
Initial denature	95	2	1
Denature	95	1	
Annealing	65-75	1	35
Extension	72	2-5	
Final Extension	72	5	1

Table 6: Temperature and cycle conditions for PCR

Many variations of primer sequences and cycling parameters were tested to optimise PCR conditions, but due to the short overhangs produced by the first round of PCR, these were not sufficient to prime the next round of PCR and produce the chimeric receptor sequence. A different method was devised by identifying a restriction site specific to the overhang region and absent in the coding sequence for both α7nAChR and 5-HT$_{3A}$. This would then allow digestion of the overlap region, producing complementary ends on each sequence, to then ligate the two fragments together.

2.6.7.2. Restriction endonuclease digest

Restriction endonucleases are enzymes typically found in bacteria to digest foreign DNA as a defence mechanism, and have been identified as critical tools in many applications such as cellular analysis, protein expression and purification, epigenetics, DNA modification and cloning. These enzymes recognise specific palindromic sequences of 4 to 8 nucleotides, termed restriction sites and cleave the DNA at these sites. The enzymes can produce 'blunt' ends, where the double-stranded DNA is cut in the same place on both strands; or they can produce 'sticky' ends, where the strands are cut in different places, creating an overhang. Different DNA fragments which are cut with the same restriction enzyme have complementary ends and can be joined together.

An MreI restriction site was identified specifically in the 5-HT$_{3A}$ receptor sequence at the overlap region for constructing the chimera. As the restriction site was present in the 5-HT$_{3A}$ receptor sequence, the 5-HT$_{3A}$ fragment could be cleaved directly out of its plasmid vector. The α7nAChR did not contain the MreI site, therefore the site was introduced by PCR by using the α7 FF primer (see table 4) and a chimeric reverse primer (CRev1, see table 4) containing the 5-HT$_{3A}$ overhang and the MreI site. The α7 fragment would then contain the restriction sites BamHI at the 5' end and MreI at the 3' end. Table 7 shows the cleavage sites for the enzymes used during experiments.

Endonuclease	Sequence Cleaved
Fastdigest MreI (Thermo Scientific, FD2024)	5'-CG/CCGGCG-3' 3'-GCGGCC/GC-5'
Fastdigest BamHI (Thermo Scientific, FD0054)	5'-GG/ATCC- 3' 3'-CCTAG/G-5'
Fastdigest XbaI (Thermo Scientific, FD0684)	5'-T/CTAGA-3' 3'-AGATC/T- 5'

Table 7: Enzyme restriction site recognition

The Fastdigest enzymes are restriction enzymes artificially altered to cleave 1µg of DNA in 5 minutes. The MreI restriction site was found to cleave the entire chimeric sequence once at the crossover point between $\alpha 7$ nicotinic acetylcholine sequence and 5-HT$_3$A sequence. This enzyme was used to cleave the PCR products obtained from overlap extension PCR to then ligate the two fragments together and form the full length chimeric sequence.

α7nAChR PCR Product Digest: Fragment 1	
10X Fastdigest buffer	5 µL
DNA	Up to 200 ng
BamHI (Thermo Scientific, FD0684)	1 µL
MreI (Thermo Scientific, FD2024)	1 µL
ddH$_2$O	Final volume of 50 µL

Table 8 : Components for a digest of the α7nAChR PCR product

pcDNA3.1-5HT$_{3A}$ Digest	
10X Fastdigest buffer	5 µL
DNA	5 µg
MreI (Thermo Scientific, FD2024)	5 µL
XbaI (Thermo Scientific, FD0684)	5 µL
ddH$_2$O	Final volume of 50 µL

Table 9: Components for a digestion of pcDNA3.1-5HT$_{3A}$

The digest reactions were incubated at 37°C for 10 minutes, followed by heat inactivation at 80°C for 5 minutes. Digested fragments were then separated by agarose gel electrophoresis to remove the small digested fragments, to prevent re-ligation in further experiments.

2.6.7.3. DNA Ligation

DNA ligation is the process of joining nucleotides together using a catalyst. T4 DNA ligase, obtained from bacteriophage T4, catalyses the formation of phosphodiester bonds between nucleotides, thus joining fragments together. The plasmid vector pcDNA3.1, and the chimeric nucleic acid sequence previously underwent a double digest with XbaI and BamHI, creating cohesive ends. The plasmid vector pcDNA3.1 (Invitrogen) and the chimeric $\alpha7_{V201}5HT_3A$ receptor sequence were added at different molar ratios (vector : insert) to optimise the ligation of the chimera into the vector, and incubated with 0.3 units of T4 DNA ligase (Promega, M1801). The reaction was incubated at 4°C overnight. The ligation reaction components are described in the table below, and the expected size of the plasmid with the chimeric insert was 7.3 kb.

Ligation Reaction	
Vector DNA	100 ng
Insert DNA	17 ng
T4 Ligase 10X Buffer	1 µL
T4 DNA Ligase (Weiss units)	0.3 units
Total Reaction Volume made up with dH$_2$O	10 µL

Table 10: Components for a ligation reaction

To ensure successful ligation, some of the product was digested with the same restriction enzymes used to digest the chimeric insert (see section 2.6.7.2.), the undigested and digested product were run in a 1% agarose gel, against Hyperladder I™ (Bioline). The band marking the successfully ligated insert in the plasmid was apparent between the 6 and 8 kb marker in Hyperladder I™; the undigested product as a smeary band, due to the supercoiled nature of the plasmid, and the digested plasmid as a clear band with no smears, as the restriction enzymes had linearised the product.

2.6.8. Use of Bacterial Hosts

2.6.8.1. Bacterial Culture

All preparations and handling bacterial cultures were carried out in a sterile environment under a Bunsen burner. Culture medium was autoclaved to preserve sterility. Liquid bacteria cultures were grown at 37°C, in an elliptical incubator (New Brunswick, Innova 4400), shaking at 225-250 rpm, in 25 g/L Luria-Bertani (LB) medium (Sigma, L3397), supplemented with 100 µg/mL ampicillin (Invitrogen, 11593027). Solid phase bacterial cultures were grown on 2% (w/v) agar (Sigma, A5306), dissolved and autoclaved in LB medium, then supplemented with 100 µg/mL ampicillin once cooled and set in sterile agar plates.

Luria Bertani Medium	
Tryptone	10 g/L
Yeast Extract	5 g/L
NaCl	5 g/L

Table 11: Composition of Luria-Bertani Medium

2.6.8.2. Bacterial Transformation

Bacterial transformation is a naturally occurring process which allows bacteria to exchange DNA, adapt and evolve, in situations such as damaged DNA. Bacteria which can accept foreign DNA are termed competent. Supercompetent XL10 Gold® E. coli (Agilent, 200314) were used to grow large quantities of DNA for further molecular biology.

To transform the bacteria, 200 µL supercompetent XL10 Gold E. coli (Agilent, 200314) were incubated with approximately 50 ng of the recombinant DNA on ice for 20 minutes. They were then heat shocked for 45 seconds in a water bath at 42˚C and then placed on ice for a further 3 minutes. The bacteria were then incubated in 500 µL LB broth at 37˚C, in the elliptical incubator for 1.5 hours. Each bacterial transformation was spread on an agar plate, left to dry, and incubated overnight at 37˚C.

2.6.8.3. DNA Extraction and Purification from Bacterial Cells

Large scale extraction and purification of DNA from bacteria generates a high yield of DNA, which is useful for mammalian cell transfections. Transformed bacteria are grown in large volumes in overnight bacterial cultures, to then undergo alkaline lysis with sodium dodecyl sulphate (SDS), a method developed by Birnboim and Doly (1979). Commercially available kits (Qiagen Plasmid Maxi Kit, 12163) rely on this basis to purify plasmid DNA from bacterial cells.

Single colonies without microsatellites were selected from the agar plates and inoculated in 5 mL LB medium supplemented with ampicillin and incubated at 37˚C for approximately 8

hours. The cultures were then tipped into Erlenmeyer flasks containing 300 mL LB broth and 100 µg/mL ampicillin. The flasks were incubated in the elliptical incubator at 37˚C overnight.

The following day, the bacterial cultures had exponentially grown and filled the flasks. The contents of the flasks were divided into 50 mL centrifuge tubes and the cells harvested at 4000 x g for 10 minutes. The supernatant medium was then discarded, then the cells were resuspended in 10 mL resuspension buffer containing RNase A (see table number 12) until no cell clumps remained. The cells were then lysed with 10 mL lysis buffer, mixed by inverting the tubes and incubated at room temperature for 5 minutes. The Qiagen® Plasmid Maxi Kit contains LyseBlue, a colour indicator which turns the cell suspension blue when the lysis buffer has been homogenously mixed. 10 mL chilled precipitation buffer was added to the lysate, mixed until the suspension became colourless, then incubated on ice for 20 minutes. The lysate was then transferred to Beckman Coulter polycarbonate centrifuge tubes (Beckman Coulter, 41121703), and centrifuged at 18 000 x g for 30 minutes at 4°C in an ultracentrifuge (Beckman Coulter) to remove the precipitated genomic DNA, proteins and cell debris in SDS. The clear supernatant solution was isolated, and then centrifuged again at 18 000 x g for 15 minutes at 4°C. The clear supernatant was loaded onto a pre-equilibrated maxiprep column, and allowed to enter the resin matrix by gravity flow. The column was then washed with 30 mL wash buffer to remove most contaminants, and then washed a second time to remove carbohydrates.

The DNA bound to the resin was eluted in 15 mL elution buffer, and precipitated by adding 10.5 mL (0.7 volumes) of room temperature isopropanol. The preparation was mixed and centrifuged at $\geq$ 15 000 x g for 30 minutes at 4°C. The supernatant was discarded, the DNA pellet was washed with 5 mL of room temperature ethanol and centrifuged at $\geq$ 15 000 x g for

10 minutes at 4°C. After removing the supernatant and air-drying the pellet, it was resuspended in 100-500 µL nuclease-free water. The purified DNA could then be quantified by microvolume spectroscopy as described in section2.6.3., and then used for downstream molecular biology.

Buffer	Composition
Resuspension Buffer P1	50 mM Tris-HCl, pH 8.0 10 mM EDTA 100 µg/mL RNase A
Lysis Buffer P2	200 mM NaOH 1% (w/v) SDS 0.1% (v/v) LyseBlue
Precipitation Buffer P3	3.0 M Potassium acetate, pH 5.5
Wash Buffer QC	50 mM MOPS, pH 7.0 15% (v/v) Isopropanol 1.0M NaCl
Elution Buffer QF	50 mM Tris-HCl, pH 8.5 1.25 M NaCl 15% (v/v) Isopropanol

Table 12: Composition of the Qiagen® Plasmid Maxi Kit Buffers

CHAPTER 3: RESULTS

3.1. 5-Chloroindole Potentiates Full and Partial Agonist Responses
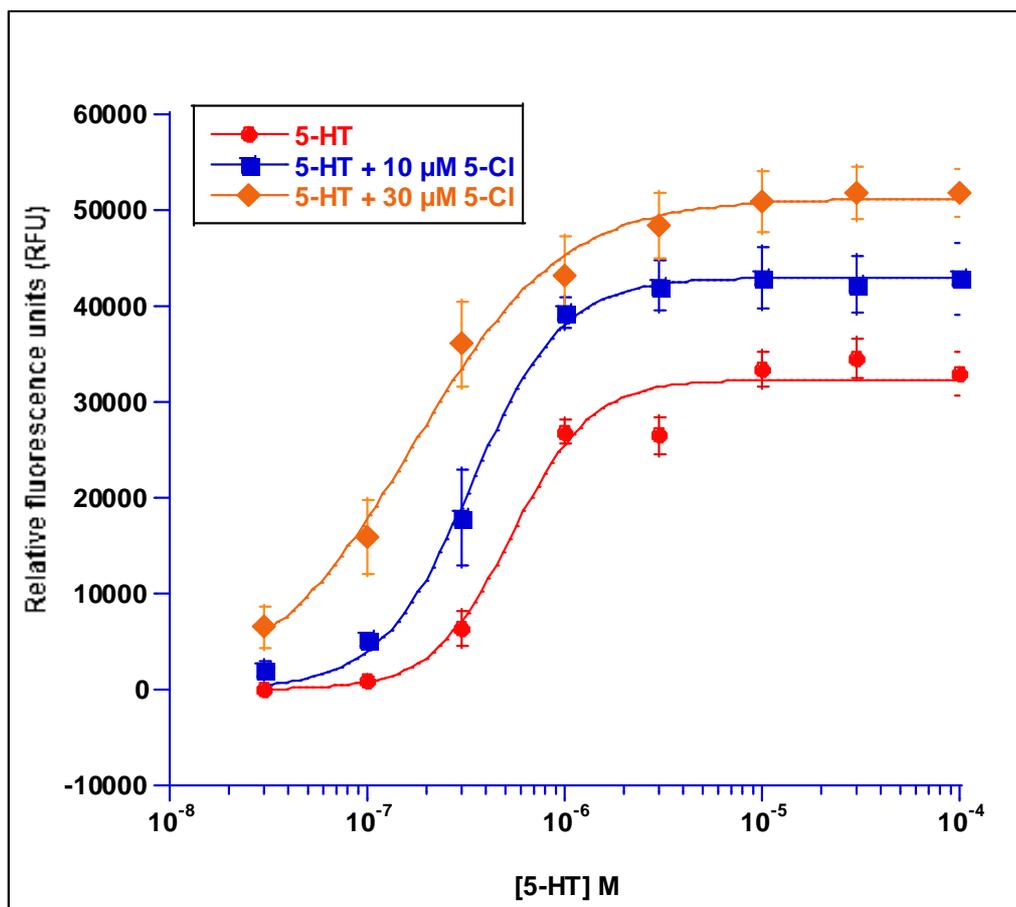
Figure 9: Ability of 10 and 30 µM 5-chloroindole to potentiate the intracellular Ca^{2+} concentration in response to 5-HT in HEK293 cells stably expressing the human 5-HT$_{3A}$ receptor, shown in relative fluorescence units. These data are representative of three independent experiments.
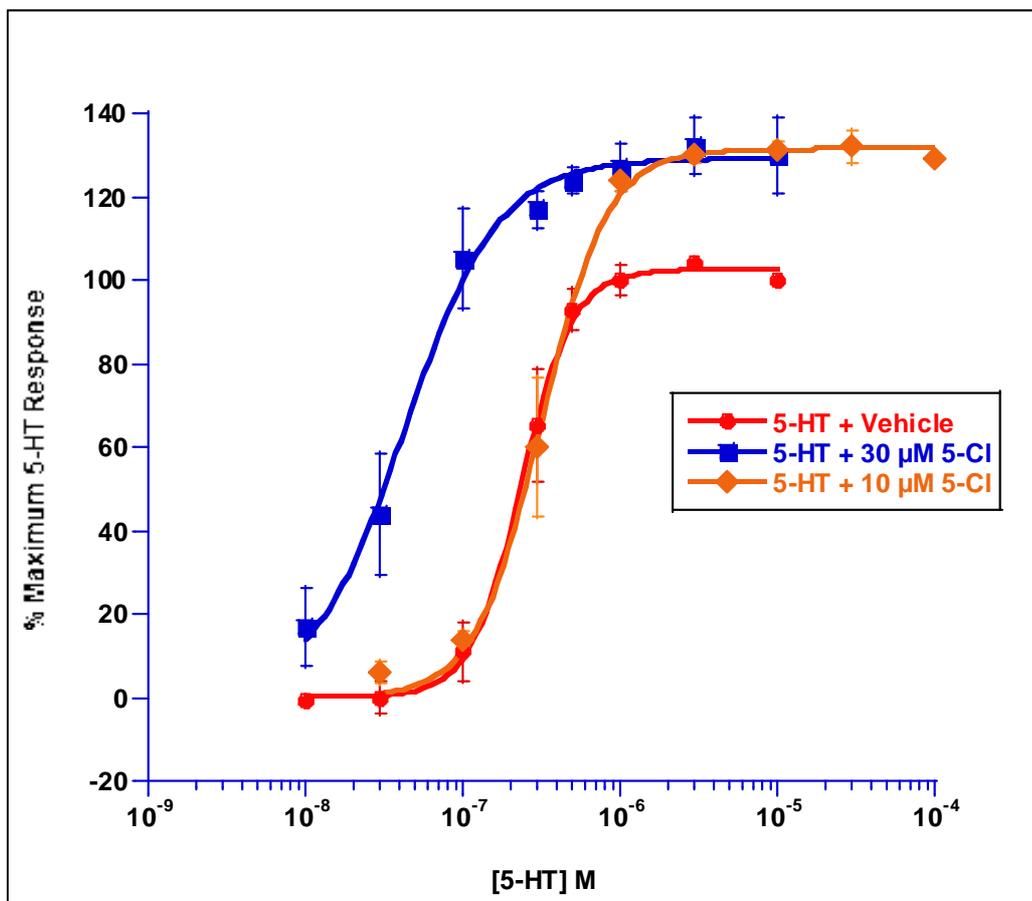
Figure 10: Concentration-response curve from intracellular calcium in HEK293 cells stably expressing the human 5-HT$_{3A}$ receptor. Error bars are mean ± standard error of the mean (SEM) of 3 independent experiments.

Results from intracellular calcium studies, as shown by the representative response curve in figure 9, showed that the concentration of intracellular calcium (shown in relative fluorescence units, RFU) reached a maximum fluorescence at approximately 30000 RFU. 5-Cl increased the maximal level of fluorescence, as well as decreasing the concentration of 5-HT required to elicit an equal level of fluorescence. Figure 10 shows the responses relative to maximal 5-HT responses. The maximal 5-HT response was increased by approximately 30% in the presence of 5-Cl and a leftward shift in the dose response could also be seen in the presence of 30 µM 5-Cl, showing a decrease in the EC$_{50}$ of 5-HT in the presence of 5-Cl.

To study allosteric properties of 5-Cl, [³H]-granisteron competition binding studies were performed to explore the effects of 5-Cl on full and partial agonist activity at the human 5-HT$_{3A}$ receptor.
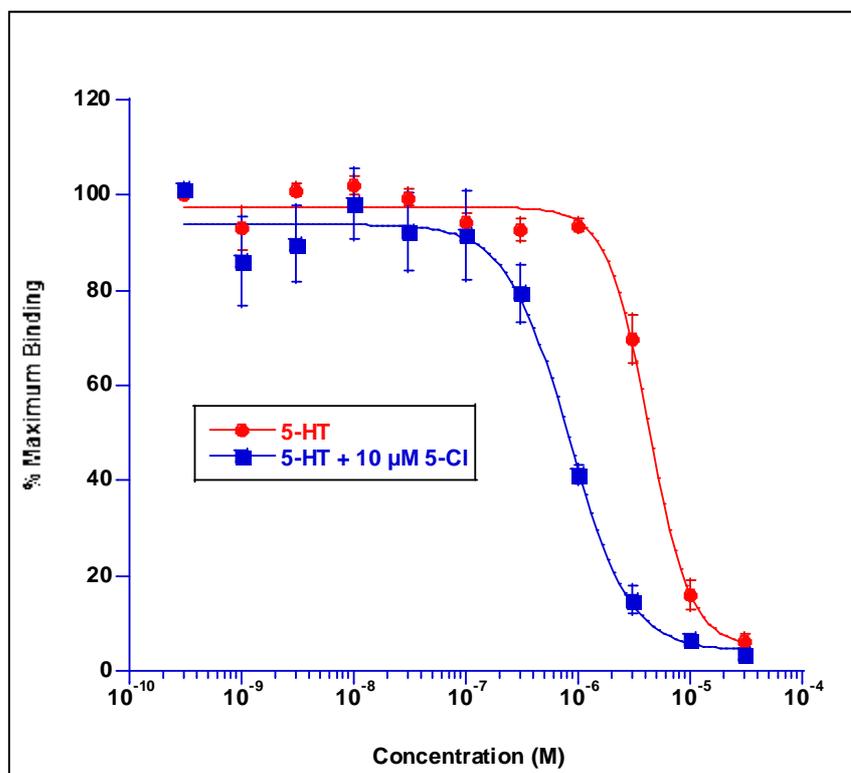
Figure 11: Competition of 5-HT for [³H]-granisetron in the absence and presence of 10 µM 5-Cl in the human 5-HT$_{3A}$ receptor. Error bars represent mean ± SEM. n=3

	pKi ± SEM	Hill number ± SEM
5-HT	5.67 ± 0.18	2.44 ± 0.14
5-HT + 10 µM 5-Cl	6.38 ± 0.22	1.65 ± 0.19

Table 13: pKi and hill numbers extrapolated from curve fit equations from graphs such as in figure 11. Data are mean ± SEM. N=3.

Figure 11 shows the competition of 5-HT with [3H]-granisteron for the 5-HT$_{3A}$ receptor. There was no difference in maximum binding in the absence and presence of 10 µM 5-Cl. 10 µM 5-Cl did however cause the leftward shift in the dose response, suggesting an increase in the binding affinity of the receptor for 5-HT. This increase in affinity was however not significant, as shown in table 13. There was also no difference between hill numbers.
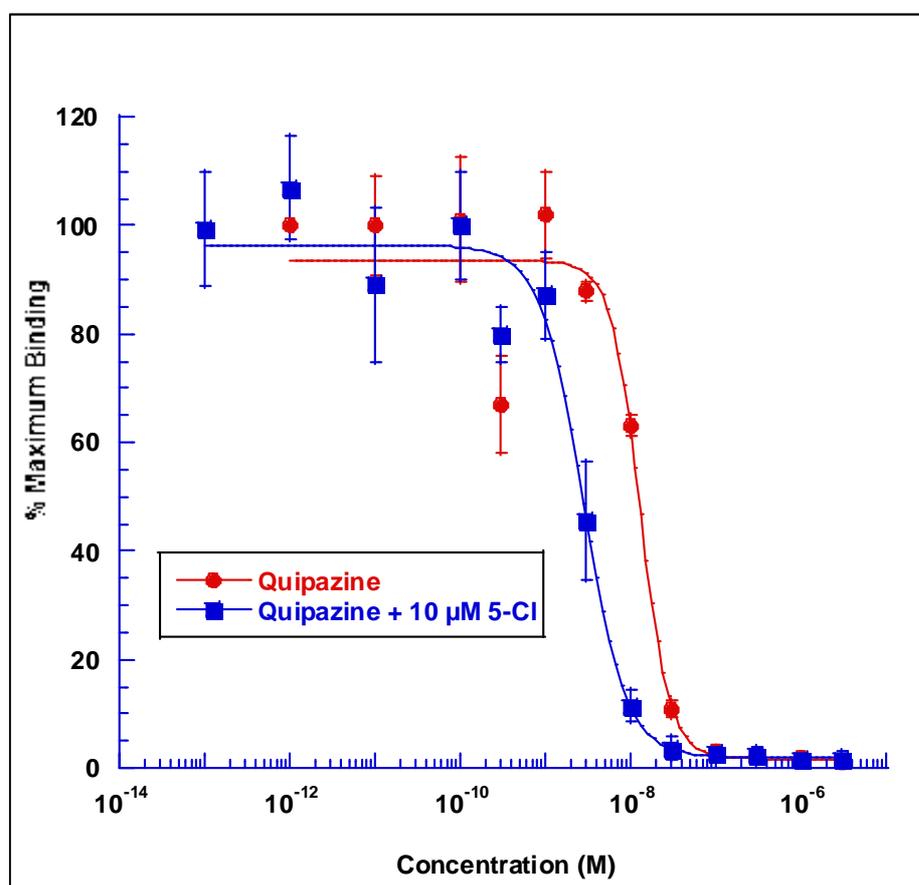
Figure 12: Competition of quipazine for [3H]-granisetron in the absence and presence of 10 µM 5-Cl in the h5-HT$_{3A}$ receptor. Error bars represent mean ± SEM. n=4

	pKi ± SEM	Hill number ± SEM
Quipazine	8.13 ± 0.06	1.44 ± 0.24
Quipazine + 10 μM 5-Cl	8.97 ± 0.06	1.55 ± 0.27

Table 14: pKi and hill numbers extrapolated from curve fit equations from graphs such as in figure 12. Data are mean ± SEM. N=3

Figure 12 shows the competition of quipazine, a partial agonist of the 5-HT$_{3A}$ receptor, with [^{3}H]-granisteron for the 5-HT$_{3A}$ receptor. There was also no difference in maximum binding in the absence and presence of 10 μM 5-Cl. 5-Cl also appeared to cause a leftward shift of the dose response curve. A small increase in quipazine binding affinity could be seen in table 14, although this was not significant.
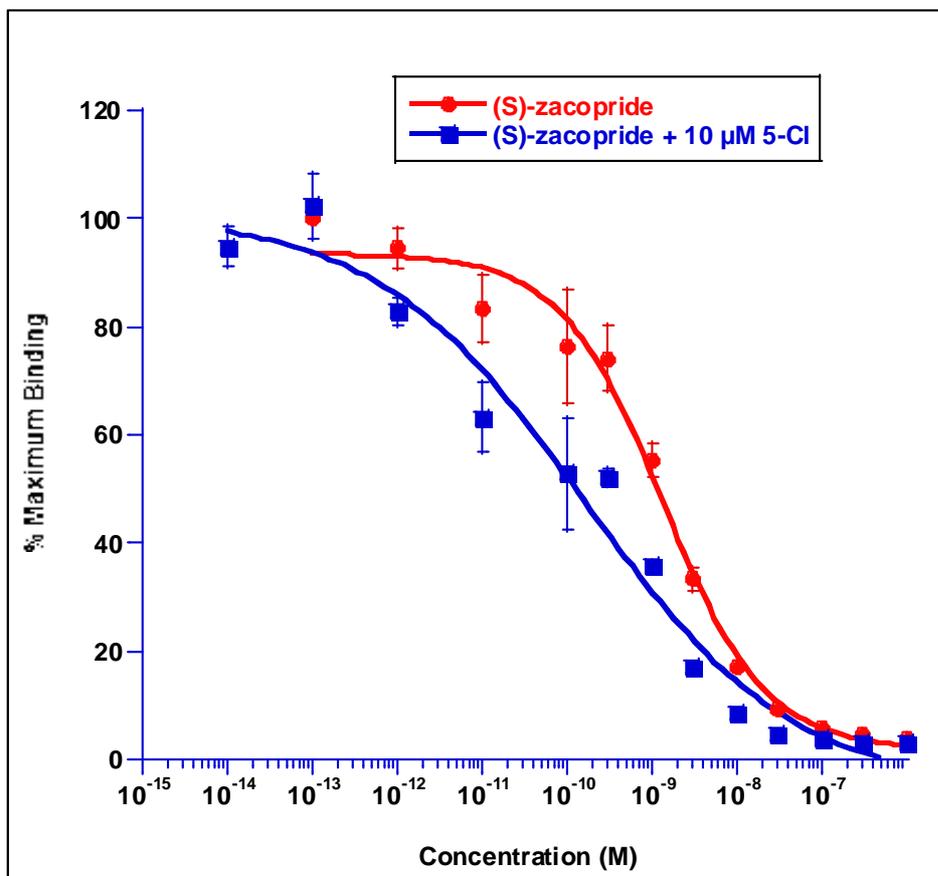
Figure 13: Competition of (S)-zacopride for [³H]-granisetron in the absence and presence of 10 µM 5-Cl in the h5-HT$_{3A}$ receptor. Error bars represent mean ± SEM. n=4

	pKi ± SEM	**Hill number ± SEM**
(S)-zacopride	9.07 ± 0.05	0.79 ± 0.08
(S)-zacopride + 10 µM 5-Cl	9.27 ± 0.41	0.58 ± 0.12

Table 15: pKi and hill numbers extrapolated from curve fit equations from graphs such as in figure 13. Data are mean ± SEM. N=3

Figure 13 shows the competition of (S)-zacopride, a partial agonist of the 5-HT$_{3A}$ receptor, with [3H]-granisteron. There was also no difference in maximum binding in the absence and presence of 10 µM 5-Cl. 5-Cl also appeared to cause a leftward shift of the dose response curve. The appearance of the dose response curve seems different to that of 5-HT and quipazine, as the curve appears flattened, as shown by a lower hill number (see table 15). There was also no significant increase in (S)-zacopride binding affinity for the 5-HT$_{3A}$ receptor.

3.2.   5-(Trifluoromethyl)indole

5-(trifluoromethyl)indole (5-TFMI) is a halogenated indole derivative, similar in structure to 5-Cl. Preliminary FlexStation analyses showed 5-TFMI potentiated 5-HT-mediated (300 nM) calcium influx, but had no effect on intracellular calcium levels when applied alone (data not shown). [3H]-granisetron competition binding studies were performed to determine orthosteric or allosteric functions.
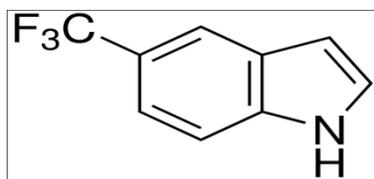
Figure 14: Chemical structure of 5-(trifluoromethyl)indole. Image taken from Sigma Aldrich.
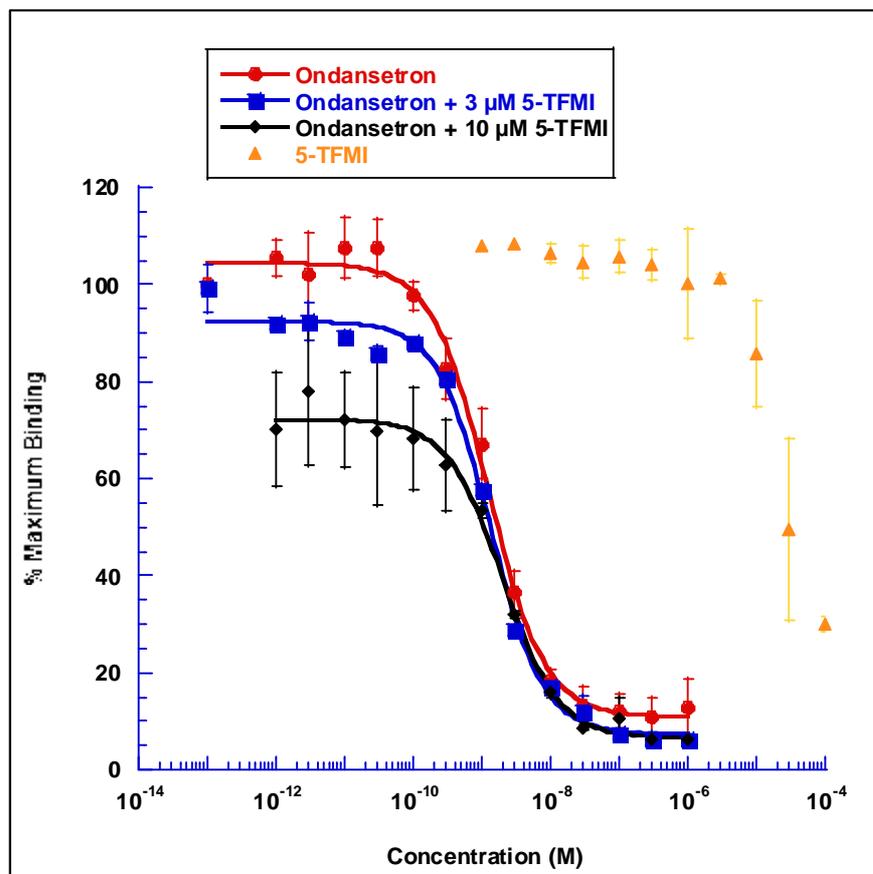
Figure 15: Lack of competition of 5-TFMI with [³H]-granisetron (orange) and lack of effect of 5-TFMI (3 and 10 µM) on ondansetron competition with [³H]-granisetron for the h5-HT$_{3A}$ receptor (blue and black). Error bars represent mean ± SEM. n=3

	pKi ± SEM	Hill number ± SEM
Ondansetron	9.04 ± 0.03	1.06 ± 0.16
Ondansetron + 3 µM 5-TFMI	9.01 ± 0.02	1.04 ± 0.12
Ondansetron + 10 µM 5TFMI	8.89 ± 0.17	0.91 ± 0.07

Table 16: pKi and hill coefficients extrapolated from curve fits in [³H]-granisetron competition binding with ondansetron experiments, as in figure 15. Data are mean ± SEM, n=3.

In [3H]-granisetron competition studies, 5-TFMI alone showed no competition for the 5-HT$_{3A}$ receptor up to 3 µM (figure 15). At concentrations higher than 10 µM, 5-TFMI appeared to compete with [3H]-granisetron. When observing the effects of 5-TFMI on antagonist (ondansetron, figure 15, blue and black traces) binding, the curves in the presence of 3 and 10 µM 5-TFMI showed no leftward shift of the dose-response curve. However, a decrease in total binding could be observed. There was no significant effect of 5-TFMI on 5-HT$_{3A}$ receptor binding affinity for ondansetron, as seen in table 16.
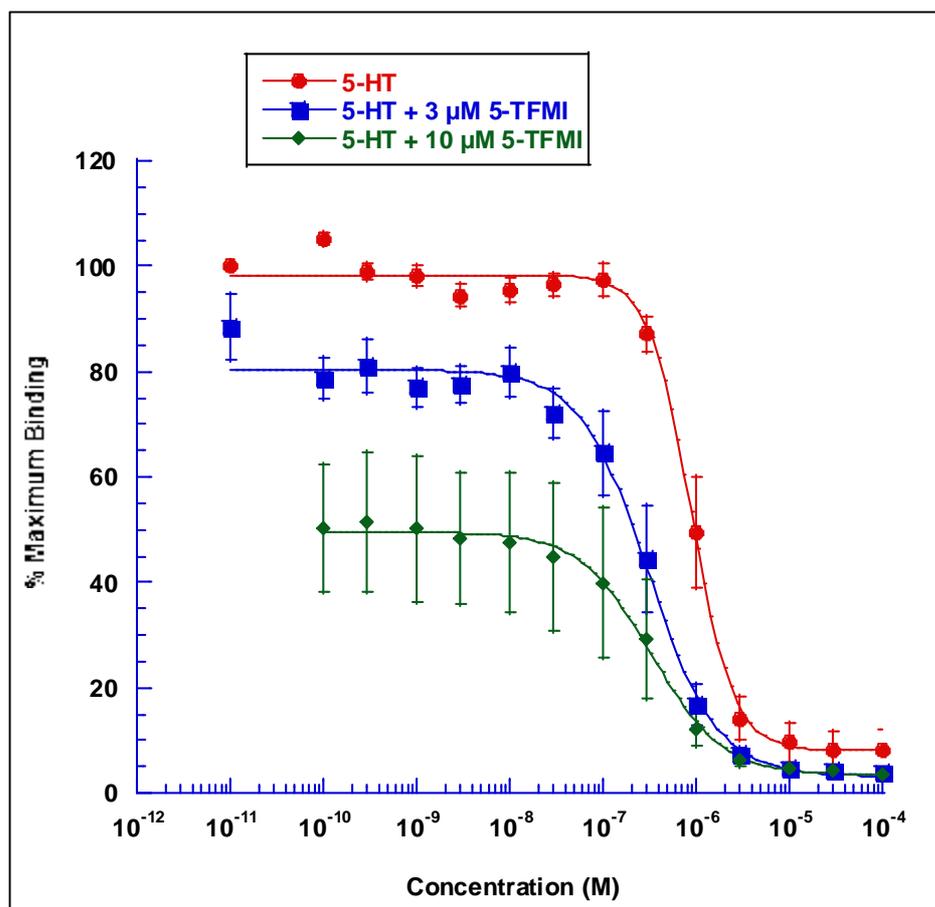
Figure 16: [3H]-granisetron competition binding with 5-HT for the human 5-HT$_{3A}$ receptor in the absence and presence of 5-TFMI (3 and 10 µM). n=4-5

	pKi	± SEM	Hill number	± SEM
5-HT	6.19	± 0.06	2.38	± 0.22
5-HT + 3µM 5-TFMI	6.64	± 0.13*	1.40	± 0.21
5-HT + 10µM 5-TFMI	6.89	± 0.11**	1.06	± 0.27*

Table 17: pKi and hill coefficients extrapolated from curve fits in [^{3}H]-granisetron competition binding with 5-HT experiments, as in figure 16. Data are mean ± SEM, n=4-5. Mann Whitney test, *p<0.05, **p<0.01

When observing the effects of 5-TFMI on 5-HT binding (figure 16), 3 and 10 µM 5-TFMI significantly increased the binding affinity of the 5-HT3A receptor for 5-HT (table17), as shown by a leftward shift of the dose response curve. However, 5-TFMI also caused a marked decrease in total binding.
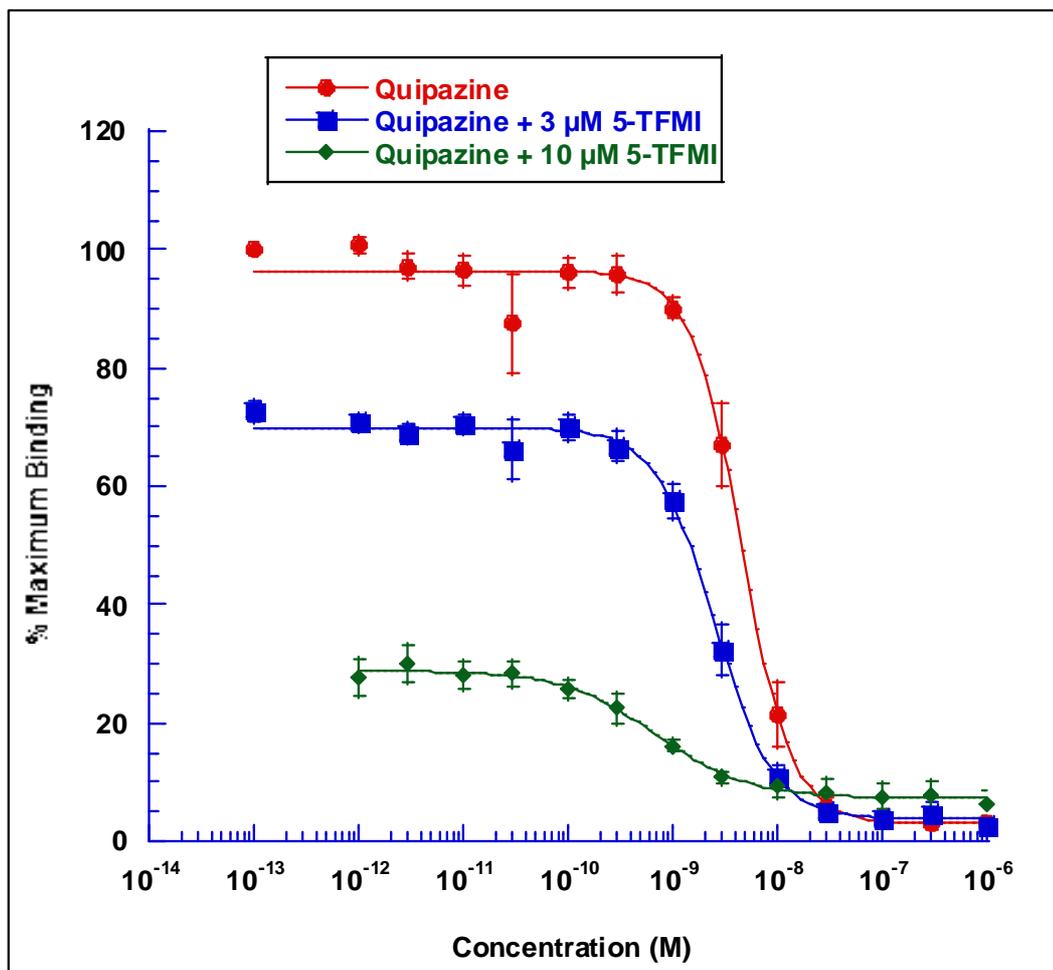
Figure 17: [³H]-granisetron competition binding of quipazine for the human 5-HT$_{3A}$ receptor in the absence and presence of 5-TFMI (3 and 10 µM). n=3-4

	pKi	± SEM	Hill number	± SEM
Quipazine	8.48	± 0.07	2.11	± 0.24
Quipazine + 3µM 5-TFMI	8.71	± 0.08	1.68	± 0.07
Quipazine + 10µM 5-TFMI	9.58	± 0.25**	1.06	± 0.19 **

Table 18: pKi and hill coefficients extrapolated from curve fits in [^{3}H]-granisetron competition binding with quipazine experiments, as in figure 17. Data are mean ± SEM, n=3-4. Mann Whitney test, **p<0.01

Figure 17 shows the effects of 3 and 10 µM 5-TFMI on quipazine competition binding. A leftward shift can be observed at both concentrations of the PAM, although the increase in binding affinity was only significant at 10 µM 5-TFMI (table 18). However, 5-TFMI also caused a marked decrease in total binding, causing maximum binding to fall to 20% of the maximum quipazine response in the presence of 10 µM 5-TFMI.
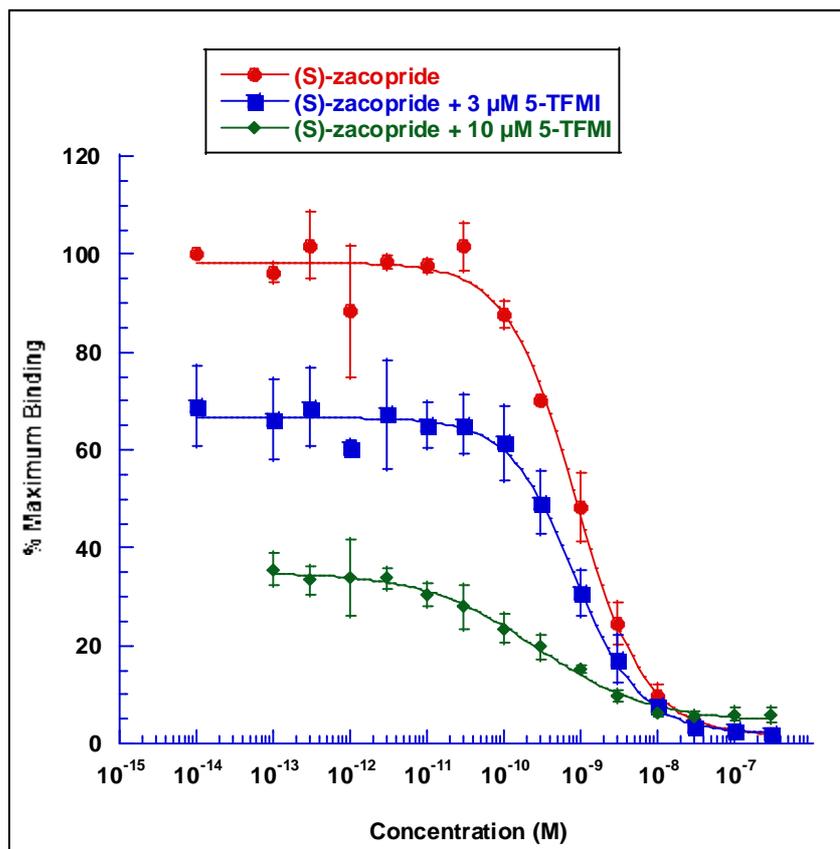
Figure 18: [^{3}H]-granisetron competition binding of (S)-zacopride in the absence and presence of 5-TFMI (3 and 10 µM). n=2-5

	pKi ± SEM	Hill number	± SEM
S-zacopride	9.35 ± 0.22	1.03	± 0.12
S-zacopride + 3µM 5-TFMI	9.21 ± 0.05	1.00	± 0.08
S-zacopride + 10µM 5-TFMI	9.96 ± 0.38	1.01	± 0.15

Table 19: pKi and hill coefficients extrapolated from curve fits in [^{3}H]-granisetron competition binding with quipazine experiments, as in figure 17. Data are mean ± SEM, n=2-5.

Figure 18 shows the effects of 5-TFMI on (S)-zacopride competition binding with [3H]-granisetron for the 5-HT$_{3A}$ receptor. There was no significant difference (table 19) in (S)-zacopride binding affinity in the presence of 5-TFMI, although this could have been affected by the decrease in maximum binding with increasing concentrations of the PAM.

These data show 5-TFMI appears to increase the binding affinity of full and partial agonists, but it also seems to affect maximum binding. This suggests 5-TFMI plays a dual role in 5-HT$_{3A}$ receptor binding.

3.3.   5-Bromoindazole and 5-Bromo-benzimidazole

5-bromoindazole (5-BI) and 5-bromo-benzimidazole (5-BBI) are halogenated indole derivatives, differing only in the position of a nitrogen atom (see figures 19 and 20). Studying the pharmacological characteristics of these compounds could help understand the core structures necessary for allosteric modulation.
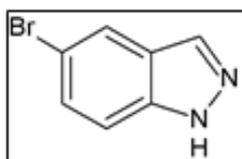
Figure 19: 5-bromoindazole
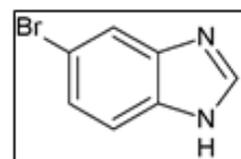
Figure 20: 5-bromo-benzimidazole

Previous work in Professor Barnes' lab showed that 5-BI stimulated calcium influx at 30 µM and 100 µM in the presence of 300 nM 5-HT, suggesting it could be a positive allosteric modulator (figure 21 left, Dr G. Gillian Grafton, Barnes lab). 5-BBI on the other hand, was shown to decrease intracellular calcium levels, suggesting it could be either an antagonist or a negative allosteric modulator (figure 21, right). [3H]-granisetron competition studies were performed to characterise orthosteric or allosteric properties.
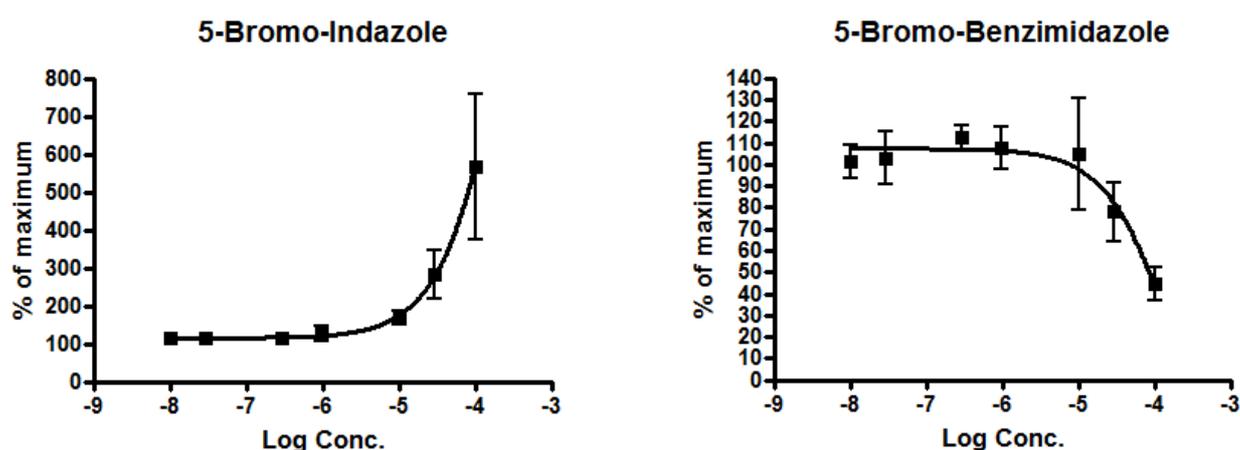
Figure 21: **Left** : Ability of 5-BI to potentiate the response evoked by 300 nM 5-HT. **Right** : Ability of 5-BBI to decrease the response evoked by 300 nM 5-HT. Error bars represent SEM. N=3. Unpublished data, experiments performed by Dr Gillian Grafton in the Barnes lab.
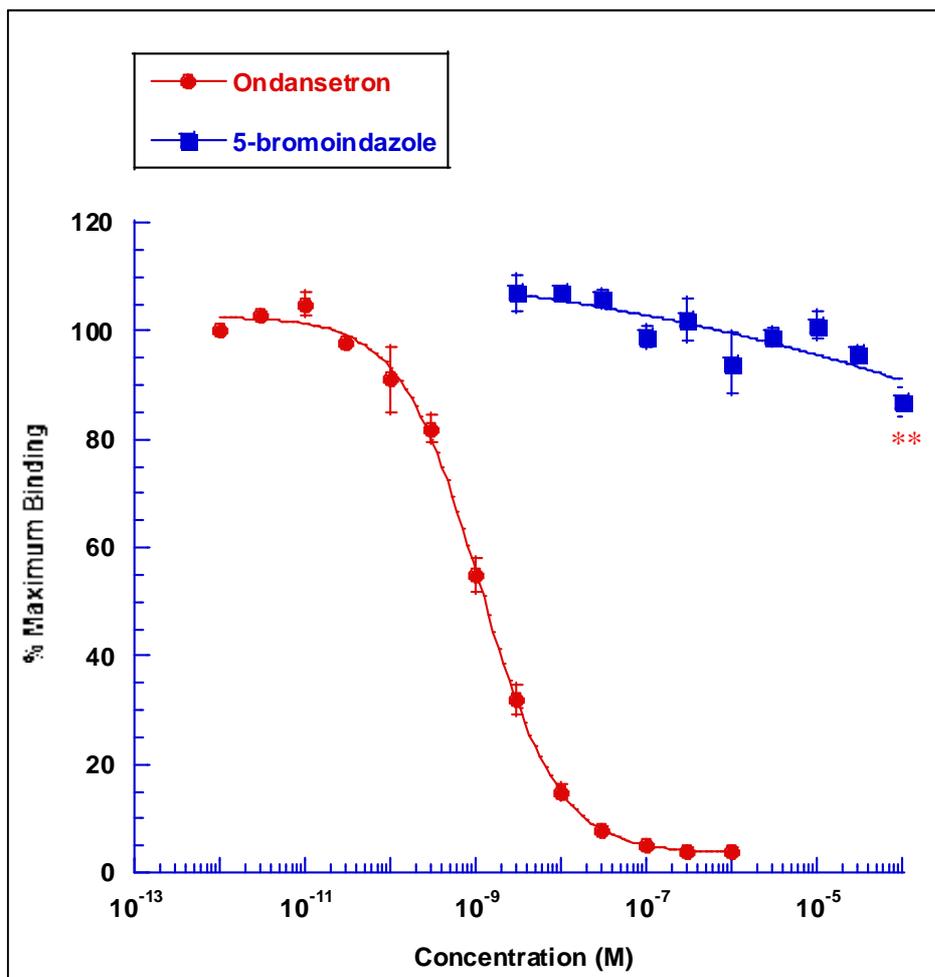
Figure 22: [^{3}H]-granisetron competition binding of ondansetron (red) and 5-bromoindazole (blue) for the human 5-HT$_{3A}$ receptor. Data represent mean ± SEM. n=3. Red * show significant differences between data points from the first three data points (ANOVA). ** p<0.01

Figure 22 shows competition radioligand binding of 5-BI compared to ondansetron as a control. There was little competition of 5-BI with [^{3}H]-granisetron for the 5-HT$_{3A}$ receptor up to 10 µM. At concentrations of 30 µM and above, the total binding appears to decrease, suggesting competition, although the decrease was only significant at 100 µM 5-BI.
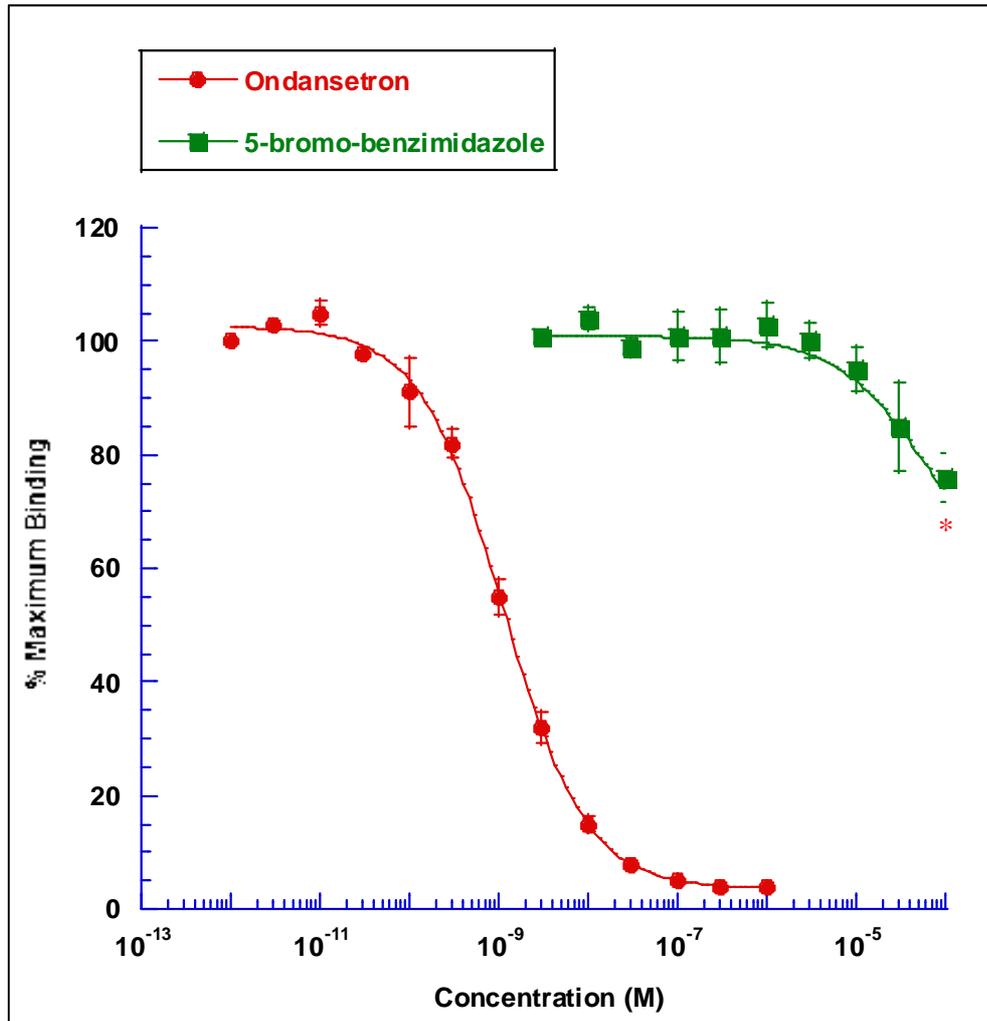
Figure 23: [^{3}H]-granisetron competition binding of ondansetron (red) and 5-bromobenz-imidazole (green) for the human 5-HT$_{3A}$ receptor. Data represent mean ± SEM. n=3. Red * show significant differences between data points from the first three data points (ANOVA). * p<0.05

Figure 23 shows competition radioligand binding of 5-BBI compared to ondansetron as a control. 5-BBI showed competition for the 5-HT$_{3A}$ receptor at concentrations above 3 µM, although only the data point at 100 µM 5-BBI was statistically different from baseline.

3.4. Construction of a Chimeric $\alpha7_{V201}5HT_{3A}$ Receptor

Eiselé et al. (1993) developed a series of rat/mouse chimerae possessing segments of the $\alpha7$ nicotinic acetylcholine receptor (nAChR) and the the mouse $5\text{-}HT_{3A}$ receptor. Of these receptors, the chimera containing the N-terminus of the rat $\alpha7$ nicotinic acetylcholine receptor (nAChR) and the transmembrane domains and C-terminus of the mouse $5\text{-}HT_{3A}$ receptor, joined at the 201st valine position in the receptor sequence ($\alpha7_{V201}5HT_{3A}$), showed nAChR ligand binding but displayed the pharmacology of the $5\text{-}HT_{3A}$ receptor. Unpublished studies (Grafton, Barnes lab) on the series of chimerae revealed the $\alpha7_{V201}5HT_{3A}$ chimera showed a lack of potentiating effects of 5-chloroindole on the activity of this chimeric receptor, suggesting the 5-Cl allosterc binding site is located in the N-terminus of the mouse $5\text{-}HT_{3A}$ receptor. Due to species differences in allosteric modulation of the $5\text{-}HT_{3A}$ receptor, a human/human chimeric receptor needed to be constructed to verify these findings.

The original $\alpha7$nAChR and $5\text{-}HT_{3A}$ receptor DNA fragments were sequenced to determine the exact nucleic acid sequence and design primers specific to these fragments. Tables 20 and 21 show the data obtained from using multiple primers and assembling the resulting sequences to form a full map of each receptor sequence.

```
            *   S   T   *   Y   D   S   L   *   A   S   L   E   A   T   M   R   C   S   P
722   tagagtacttaatacgactcactataggctagcctcgaggccaccatgcgctgctcgccg   781
            G   G   V   W   L   A   L   A   A   S   L   L   H   V   S   L   Q   G   E   F
782   ggaggcgtctggctggccctggccgcgtcgctcctgcacgtgtccctgcaaggcgagttc   841
            Q   R   K   L   Y   K   E   L   V   K   N   Y   N   P   L   E   R   P   V   A
842   cagaggaagctttacaaggagctggtcaagaactacaatcccttggagaggcccgtggcc   901
            N   D   S   Q   P   L   T   V   Y   F   S   L   S   L   L   Q   I   M   D   V
902   aatgactcgcaaccactcaccgtctacttctccctgagcctcctgcagatcatggacgtg   961
            D   E   K   N   Q   V   L   T   T   N   I   W   L   Q   M   S   W   T   D   H
962   gatgagaagaaccaagtttttaaccaccaacatttggctgcaaatgtcttggacagatcac   1021
            Y   L   Q   W   N   V   S   E   Y   P   G   V   K   T   V   R   F   P   D   G
1022  tatttacagtggaatgtgtcagaatatccaggggtgaagactgttcgtttcccagatggc   1081
            Q   I   W   K   P   D   I   L   L   Y   N   S   A   D   E   R   F   D   A   T
1082  cagatttggaaaccagacattcttctctataacagtgctgatgagcgctttgacgccaca   1141
            F   H   T   N   V   L   V   N   S   S   G   H   C   Q   Y   L   P   P   G   I
1142  ttccacactaacgtgttggtgaattcttctgggcattgccagtacctgcctccaggcata   1201
            F   K   S   S   C   Y   I   D   V   R   W   F   P   F   D   V   Q   H   C   K
1202  ttcaagagttcctgctacatcgatgtacgctggtttccctttgatgtgcagcactgcaaa   1261
            L   K   F   G   S   W   S   Y   G   G   W   S   L   D   L   Q   M   Q   E   A
1262  ctgaagtttgggtcctggtcttacggaggctggtccttggatctgcagatgcaggaggca   1321
            D   I   S   G   Y   I   P   N   G   E   W   D   L   V   G   I   P   G   K   R
1322  gatatcagtggctatatccccaatggagaatgggacctagtgggaatccccggcaagagg   1381
            S   E   R   F   Y   E   C   C   K   E   P   Y   P   D   V   T   F   T   V   T
1382  agtgaaaggttctatgagtgctgcaaagagccctaccccgatgtcaccttcacagtgacc   1441
            M   R   R   R   T   L   Y   Y   G   L   N   L   L   I   P   C   V   L   I   S
1442  atgcgccgcaggacactctactatggcctcaacctgctgatccctgtgtgctcatctcc   1501
            A   L   A   L   L   V   F   L   L   P   A   D   S   G   E   K   I   S   L   G
1502  gccctcgccctgctggtgttcctgcttcctgcagattccggggagaagatttccctgggg   1561
            I   T   V   L   L   S   L   T   V   F   M   L   L   V   A   E   I   M   P   A
1562  ataacagtcttactctctcttaccgtcttcatgctgctcgtggctgagatcatgcccgca   1621
            T   S   D   S   V   P   L   I   A   Q   Y   F   A   S   T   M   I   I   V   G
1622  acatccgattcggtaccattgatagcccagtacttcgccagcaccatgatcatcgtgggc   1681
            L   S   V   V   V   T   V   I   V   L   Q   Y   H   H   H   D   P   D   G   G
1682  ctctcggtggtggtgacagtgatcgtgctgcagtaccaccaccacgaccccgacggggggc   1741
            K   M   P   K   W   T   R   V   I   L   L   N   W   C   A   W   F   L   R   M
1742  aagatgcccaagtggaccagagtcatccttctgaactggtgcgcgtggttcctgcgaatg   1801
            K   R   P   G   E   D   K   V   R   P   A   C   Q   H   K   Q   R   R   C   S
1802  aagaggcccgggggaggacaaggtgcgcccggcctgccagcacaagcagcggcgctgcagc   1861
            L   A   S   V   E   M   S   A   V   A   P   P   P   A   S   N   G   N   L   L
1862  ctggccagtgtggagatgagcgccgtggccccgccgcccgccagcaacgggaacctgctg   1921
            Y   I   G   F   R   G   L   D   G   V   H   C   V   P   T   P   D   S   G   V
1922  tacatcggcttccgcggcctggacggcgtgcactgtgtcccgacccccgactctggggta   1981
            V   C   G   R   M   A   C   S   P   T   H   D   E   H   L   L   H   G   G   Q
1982  gtgtgtggccgcatggcctgctcccccacgcacgatgagcacctcctgcacggcgggcaa   2041
```

72

```
      P  P  E  G  D  P  D  L  A  K  I  L  E  E  V  R  Y  I  A  N
2042  cccccccgaggggggacccggacttggccaagatcctggaggaggtccgctacattgccaac  2101
      R  F  R  C  Q  D  E  S  E  A  V  C  S  E  W  K  F  A  A  C
2102  cgcttccgctgccaggacgaaagcgaggcggtctgcagcgagtggaagttcgccgcctgt  2161
      V  V  D  R  L  C  L  M  A  F  S  V  F  T  I  I  C  T  I  G
2162  gtggtggaccgcctgtgcctcatggccttctcggtcttcaccatcatctgcaccatcggc  2221
      I  L  M  S  A  P  N  F  V  E  A  V  S  K  D  F  A  *  A  A
2222  atcctgatgtcggctcccaacttcgtggaggccgtgtccaaagactttgcgtaagcggcc  2281
      A  S  L  *  *  G  L  M  L  R  A  D  M  I  R  Y  I  D  E  F
2282  gcttccctttagtgagggttaatgcttcgagcagacatgataagatacattgatgagttt  2341
```

Table 20: a7nACh receptor nucleic acid sequence with overlaid translated protein sequence. Restriction enzyme cleavage sites are marked in green (NotI at the 5' end and XhoI at the 3' end) in the nucleic acid sequence. In the protein sequence, the signalling peptide sequence is marked in blue and * mark stop codons. The conserved valine for the construction of the chimera and corresponding codon (position 754-756) are marked in red.

```
      N  *  Y  D  S  L  *  G  D  P  S  W  L  V  K  L  G  T  E  L
2     aattaatacgactcactataggggagacccaagctggctagttaagcttggtaccgagctc  61
      G  S  P  G  L  Q  E  F  R  G  H  E  R  Q  A  G  W  D  M  R
62    ggatcccccgggctgcaggaattccggggccacgagaggcaggctggctgggacatgagg  121
      L  A  E  G  R  Q  A  G  P  W  W  A  S  P  *  A  L  G  G  T
122   ttggcagagggcaggcaagctggcccttggtgggcctcgccctgagcactcggaggcact  181
      P  M  L  G  K  L  A  M  L  L  W  V  Q  Q  A  L  L  A  L  L
182   cctatgcttggaaagctcgctatgctgctgtgggtccagcaggcgctgctcgccttgctc  241
      L  P  T  L  L  A  Q  G  E  A  R  R  S  R  E  Q  K  L  I  S
242   ctccccacactcctggcacagggagaagccaggaggagccgagaacaaaaactcatctca  301
      E  E  D  L  N  T  T  R  P  A  L  L  R  L  S  D  Y  L  L  T
302   gaagaggatctgaacaccaccaggcccgctctgctgaggctgtcggattacctttttgacc  361
      N  Y  R  K  G  V  R  P  V  R  D  W  R  K  P  T  T  V  S  I
362   aactacaggaagggtgtgcgccccgtgagggactggaggaagccaaccaccgtatccatt  421
      D  V  I  V  Y  A  I  L  N  V  D  E  K  N  Q  V  L  T  T  Y
422   gacgtcattgtctatgccatcctcaacgtggatgagaagaatcaggtgctgaccacctac  481
      I  W  Y  R  Q  Y  W  T  D  E  F  L  Q  W  N  P  E  D  F  D
482   atctggtaccggcagtactggactgatgagtttctccagtggaaccctgaggactttgac  541
      N  I  T  K  L  S  I  P  T  D  S  I  W  V  P  D  I  L  I  N
542   aacatcaccaagttgtccatccccacggacagcatctgggtcccggacattctcatcaat  601
      E  F  V  D  V  G  K  S  P  N  I  P  Y  V  Y  I  R  H  Q  G
602   gagttcgtggatgtggggaagtctccaaatatcccgtacgtgtatattcggcatcaaggc  661
      E  V  Q  N  Y  K  P  L  Q  V  V  T  A  C  S  L  D  I  Y  N
662   gaagttcagaactacaagccccttcaggtggtgactgcctgtagcctcgacatctacaac  721
      F  P  F  D  V  Q  N  C  S  L  T  F  T  S  W  L  H  T  I  Q
722   ttccccttcgatgtccagaactgctcgctgaccttcaccagttggctgcacaccatccag  781
```

```
        D   I   N   I   S   L   W   R   L   P   E   K   V   K   S   D   R   S   V   F
782     gacatcaacatctctttgtggcgcttgccagaaaaggtgaaatccgacaggagtgtcttc     841
        M   N   Q   G   E   W   E   L   L   G   V   L   P   Y   F   R   E   F   S   M
842     atgaaccagggagagtgggagttgctggggggtgctgccctactttcgggagttcagcatg     901
        E   S   S   N   Y   Y   A   E   M   K   F   Y   V   V   I   R   R   R   P   L
902     gaaagcagtaactactatgcagaaatgaagttctatgtggtcatccgccggcggcccctc     961
        F   Y   V   V   S   L   L   L   P   S   I   F   L   M   V   M   D   I   V   G
962     ttctatgtggtcagcctgctactgcccagcatcttcctcatggtcatggacatcgtgggc     1021
        F   Y   L   P   P   N   S   G   E   R   V   S   F   K   I   T   L   L   L   G
1022    ttctacctgccccccaacagtggcgagagggtctctttcaaaattacactcctcctgggc     1081
        Y   S   V   F   L   I   I   V   S   D   T   L   P   A   T   A   I   G   T   P
1082    tactcggtcttcctgatcatcgtttctgacacgctgccggccactgccatcggcactcct     1141
        L   I   G   V   Y   F   V   V   C   M   A   L   L   V   I   S   L   A   E   T
1142    ctcattggtgtctactttgtggtgtgcatggctctgctggtgataagtttggccgagacc     1201
        I   F   I   V   R   L   V   H   K   Q   D   L   Q   Q   P   V   P   A   W   L
1202    atcttcattgtgcggctggtgcacaagcaagacctgcagcagcccgtgcctgcttggctg     1261
        R   H   L   V   L   E   R   I   A   W   L   L   C   L   R   E   Q   S   T   S
1262    cgtcacctggttctggagagaatcgcctggctactttgcctgagggagcagtcaacttcc     1321
        Q   R   P   P   A   T   S   Q   A   T   K   T   D   D   C   S   A   M   G   N
1322    cagaggcccccagccacctcccaagccaccaagactgatgactgctcagccatgggaaac     1381
        H   C   S   H   M   G   G   P   Q   D   F   E   K   S   P   R   D   R   C   S
1382    cactgcagccacatgggaggaccccaggacttcgagaagagcccgagggacagatgtagc     1441
        P   P   P   P   P   R   E   A   S   L   A   V   C   G   L   L   Q   E   L   S
1442    cctcccccaccacctcgggaggcctcgctggcggtgtgtgggctgctgcaggagctgtcc     1501
        S   I   R   Q   F   L   E   K   R   D   E   I   R   E   V   A   R   D   W   L
1502    tccatccggcaattcctggaaaagcgggatgagatccgagaggtggcccgagactggctg     1561
        R   V   G   S   V   L   D   K   L   L   F   H   I   Y   L   L   A   V   L   A
1562    cgcgtgggctccgtgctggacaagctgctattccacatttacctgctagcggtgctggcc     1621
        Y   S   I   T   L   V   M   L   W   S   I   W   Q   Y   A   *   V   G   T   A
1622    tacagcatcaccctggttatgctctggtccatctggcagtacgcttgagtgggtacagcc     1681
        Q   W   R   R   G   Y   S   P   G   *   V   G   T   E   D   F   C   L   G   P
1682    cagtggaggaggggtacagtcctggttaggtggggacagaggatttctgcttaggcccc     1741
        S   G   P   R   E   C   Q   G   H   F   Q   D   T   D   K   V   P   C   P   V
1742    tcaggacccagggaatgccagggacattttcaagacacagacaaagtcccgtgccctgtt     1801
        S   N   A   N   S   S   Q   Q   S   Q   A   K   V   *   T   L   P   P   K   T
1802    tccaatgccaattcatctcagcaatcacaagccaaggtctgaacccttccaccaaaaact     1861
        G   C   S   R   P   L   H   P   C   P   T   P   S   S   S   P   W   L   *   N
1862    gggtgttcaaggcccttacacccttgtcccaccccccagcagctcaccatggctttaaaac     1921
        M   L   S   *   I   R   R   N   S   G   T   P   *   V   H   S   S   C   G   L
1922    atgctctcttagatcaggagaaactcgggcactccctaagtccactctagttgtggactt     1981
        F   P   I   D   P   H   L   N   K   G   L   W   N   S   I   S   S   L   S   I
1982    ttccccattgaccctcacctgaataagggactttggaattcgatatcaagcttatcgata     2041
        P   S   T   S   S   M   H   L   E   G   P
2042    ccgtcgacctcgagcatgcatctagagggccct     2074
```

Table 21: 5-HT$_{3A}$ receptor nucleic acid sequence with overlaid translated protein sequence. Restriction enzyme cleavage sites are marked in green (BamHI at the 5' end and XbaI at the 3' end) in the nucleic acid sequence. In the protein sequence, the signalling peptide sequence is marked in blue and * mark stop codons. The conserved valine for the construction of the chimera and corresponding codon (position 941-943) are marked in red at positions.

The first round of overlap extension PCR was successful in obtaining the α7nAChR and 5-HT$_{3A}$ receptor megaprimers (expected bands of 721 and 1126 bp respectively), shown in figure 24. The second round of PCR using the megaprimers as templates for each other was however unsuccessful in producing a full length chimera of 1836 bp, as no band was visible in an agarose gel electrophoresis. Due to the lack of a chimeric receptor with this method, another method (introducing a common restriction site to ligate sticky ends) was attempted in parallel to optimise production.
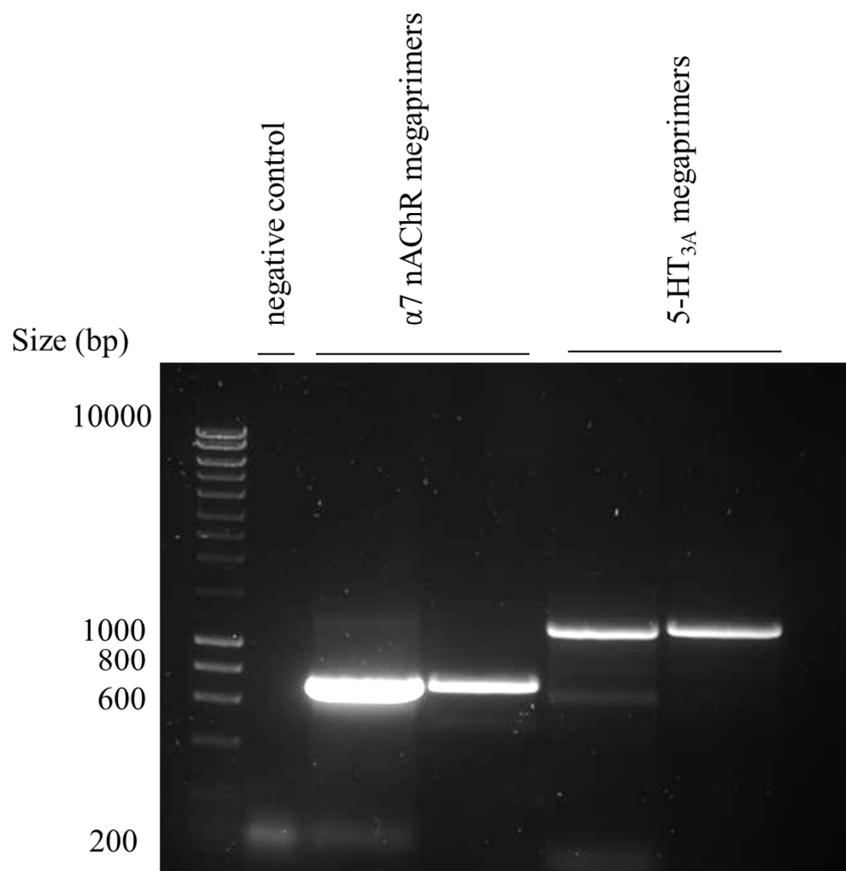
Figure 24: Products of first round of overlap extension PCR, the α$_7$ nAChR N-terminus fragment with 3' 5-HT3A overhang and the 5-HT3A C-terminal fragment with 5' α$_7$ nAChR overhang.

Restriction endonuclease digest of the plasmid vector containing the 5-HT$_{3A}$ DNA with MreI and XbaI was successful in obtaining the correct size fragment (1126 base pairs, see figure 25). PCR of the α7nAChR DNA to introduce the MreI restriction site appeared to be successful as it rendered a band of the correct size (721 bp, see figure 26). The α7nAChR fragment was then excised and digested with restriction enzymes BamHI and MreI. The ligation of these α7nAChR and 5-HT$_{3A}$ fragments appeared to succeed as a band of the correct size (1847 bp, see figure 27) was visible, although the negative control also produced a band of the same size, suggesting contamination. Subsequent amplification of the potential chimeric fragment with primers α7 FF and 3A RF did not yield any further products and DNA sequencing failed to reveal a chimeric sequence, suggesting the band was produced as a result of contamination.
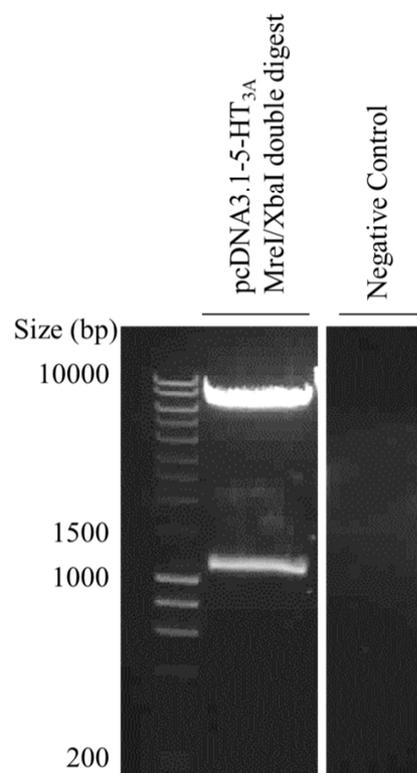
Figure 25: Double digest of pcDNA3.1-5-HT3A with MreI/XbaI
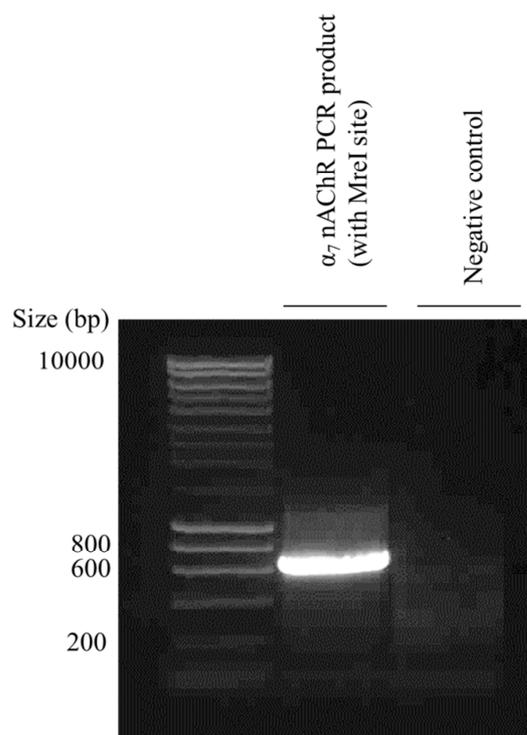
Figure 26: PCR product of α7nAChR with MreI site inserted.
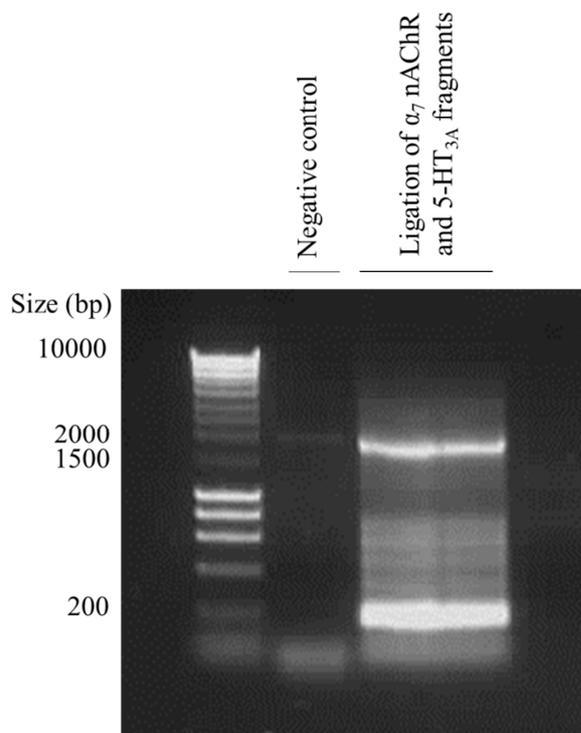
Figure 27: Ligation of α_7 nAChR and 5-HT$_{3A}$ fragment

CHAPTER 4: DISCUSSION

Experiments studying 5-chloroindole's impact upon the human 5-HT_{3A} receptor suggest it is a positive allosteric modulator, although results were not significant. Data published by Newman et al. (2013) show it is a potent positive allosteric modulator of the human 5-HT_{3A} receptor and it has served as a useful tool for characterising allosteric binding and developing novel compounds. Due to time constraints, it was not possible to complete further experiments, which could have increased the significance of the results.

5-(trifluoromethyl)indole, a halogenated indole derivative with a similar structure to 5-chloroindole, showed allosteric binding by potentiating the 5-HT response in intracellular calcium studies. Initial radioligand binding studies revealed allosteric binding due to the lack of competition with $[^{3}\text{H}]$-granisetron for the orthosteric binding site at relevant concentrations. $[^{3}\text{H}]$-granisetron competition binding studies in the presence of agonists showed positive allosteric modulation of the 5-HT_{3A} receptor by potentiating full and partial agonist responses and increasing their affinities for the 5-HT_{3A} receptor. These experiments however also revealed orthosteric binding due to 5-TFMI competing with $[^{3}\text{H}]$-granisetron and decreased the total binding of the drugs, which is contradictory to the initial results showing a lack of orthosteric binding. One possible explanation could be 5-TFMI binds to part of the orthosteric binding site and part of the allosteric binding site simultaneously. If this is the case, this would suggest the allosteric binding site is in close proximity to the orthosteric binding site in the N-terminus. Another hypothesis could be that 5-TFMI only binds to the orthosteric binding site, but causes the contributing loops to fold differently, by either stabilising the binding pocket formed by loops A, B, D and E, or to increase loop C

contraction around the agonists. This would result in agonists binding more preferentially to the same or another othosteric binding site on the receptor, or binding for longer durations and thus potentiating the agonists' responses. This is an interesting concept as it would suggest there are compounds which bind to the orthosteric site and have no action alone but increase the binding affinities of other drugs to the orthosteric site to increase the receptor response.

5-bromoindazole and 5-bromobenz-imidazole were interesting to study for their structure-activity relationships. They have shown that the structure of a compound is vital to its function and very small changes to the structure of a halogenated indole can turn a positive allosteric modulator (5-BI) into a negative allosteric modulator or antagonist.

In addition to studying the pharmacology of the allosteric binding site, locating the allosteric binding site is also important for understanding allosteric modulation. Previous studies (Corringer et al. (1998) and Kracun et al. (2008)) studying a series of rat/mouse α7nAChR/5-HT$_{3A}$ subunit chimeras showed that the α7$_{V201}$5-HT$_{3A}$ chimera, with the N-terminus of the α7nAChR and the rest of the receptor being 5-HT$_{3A}$, would bind acetylcholine, but retained the pharmacology of the 5-HT$_{3A}$ receptor. This was an interesting receptor to study for ligand binding properties. Further unpublished studies (Grafton, G., personal communication) on the same chimeric receptors revealed that of the range of chimeras, the response evoked by acetylcholine in the α7$_{V201}$5-HT$_{3A}$ chimera was not potentiated by 5-chloroindole. This would suggest the allosteric binding site of the 5-HT$_{3A}$ receptor was in the N-terminus, due to elimination of allosteric activity in the chimera. However, this chimeric receptor was a rat/mouse chimera, and as previously discussed, there are species differences (Hoyer and Middlemiss, 1989) in allosteric modulation of the 5-HT$_3$ receptor, thus requiring the construction of a human/human chimera to support these results.

I attempted to replicate the methods of Bertrand et al. (2008) using overlap extension PCR, but the overhangs produced appeared to be too short to prime the complementary strand. I attempted to elongate the primers, in order to produce a larger overhang, but to no avail. I did not use identical primers to Bertrand et al. (2008) due to the different restriction enzymes needed to insert the chimeric receptor into a plasmid vector. The PCR products I obtained had small portions of plasmid sequence due to the location of the restriction enzymes and perhaps this prevented annealing of primers or overhangs. In parallel, I attempted to cleave the sequence at the V201 region with MreI and ligate the digested fragments together. Digestion of the 5-HT$_{3A}$ receptor fragment was successful but the MreI restriction site needed to be introduced into the α7nAChR sequence by PCR, therefore it is possible this PCR was unsuccessful as the primer was not fully complementary to the α7nAChR sequence. I believe if more time had been available, the overlap extension PCR would have succeeded as I optimised parameters.

Studying the structure-activity relationship of allosteric modulators of the human 5-HT$_{3A}$ receptor will allow us to determine the pharmacophore, the core structure of a compound, and then to make smaller alterations in the structure to create potent allosteric modulators. The aim would be to develop negative allosteric modulators which will bind with high affinity to the 5-HT$_{3A}$ receptor and decrease intrinsic activity without total blockade. A negative allosteric modulator of the 5-HT$_{3A}$ receptor could have multiple therapeutic uses both centrally and peripherally. Activation of 5-HT$_3$ receptors centrally causes pro-emetic and anxiogenic effects and peripherally, stimulates peristalsis in IBS-D patients. Decreasing the activity of the 5-HT$_3$ receptor would therefore be useful in improving the treatment of symptoms without the unpleasant side effects observed during full blockade using antagonists. Determining the location and structure of the allosteric binding site could help in

developing therapeutically relevant compounds. However, allosteric modulators could be stabilising a conformational state not usually seen in the resting state of the receptor, therefore studying the structure of the receptor when bound to an allosteric modulator could also improve the development of agonists and antagonists with higher binding affinity.

CHAPTER 5: FURTHER WORK

I have outlined the importance of structure-activity relationship in this study on halogenated indole derivatives. Further work is needed on determining which structures are important for binding to the allosteric binding site, which structures determine positive allosteric modulation and which ones determine negative allosteric modulation. PAMs have proved useful for studying the pharmacology of the binding site. 5-chloroindole is a potent PAM, but 5-TFMI appears to demonstrate both orthosteric and allosteric properties. One way of determining whether 5-TFMI does bind to the orthosteric binding site would be to study [^{3}H]-granisetron competition binding of 5-TFMI (as in figure 16, yellow data points) in the absence and presence of a low concentration of 5-HT. If the total level of binding is decreased by 5-HT, this would mean 5-HT is competing with 5-TFMI for the orthosteric binding site. The functions of 5-BI and 5-BBI are determined by the position of a nitrogen atom in their structure. The grouping of all this information and further studies will ultimately define the core structure of an allosteric modulator of the human 5-HT$_{3A}$ receptor, which will bind with high affinity to the site. This will then aid in designing negative allosteric modulators with potential therapeutic use.

Constructing the human/human $\alpha7_{V201}$5-HT$_{3A}$ chimera is equally essential in supporting the data found in the rat/mouse chimera. This would confirm findings that the allosteric binding site is located in the N-terminus of the 5-HT$_{3A}$ receptor and thus mutants or knock-outs of smaller sections of the N-terminus could be constructed to determine the precise residues involved in the allosteric binding site.

Due to the recent success in obtaining the crystal structure of the mouse 5-HT$_{3A}$ receptor, this will remarkably help in progressing with studying the allosteric binding site. An interesting experiment to conduct would be a crystal soak, where the protein is crystallised and then soaked in the ligand, which will result in a ligand-protein interaction stable enough for visualisation (Hassell et al., 2007). However, Hassaine et al. (2014) discuss the fact that the co-crystallisation molecules VHH15 bind to parts of the ligand binding domain and inhibit 5-HT induced currents in electrophysiological experiments. This could therefore hinder the binding of some compounds to the orthosteric binding site but if 5-chloroindole is a PAM which binds solely to the allosteric binding site, this binding interaction could still be studied.

REFERENCES

ANDRESEN, V., MONTORI, V. M., KELLER, J., WEST, C. P., LAYER, P. & CAMILLERI, M. 2008. Effects of 5-hydroxytryptamine (serotonin) type 3 antagonists on symptom relief and constipation in nonconstipated irritable bowel syndrome: a systematic review and meta-analysis of randomized controlled trials. *Clin Gastroenterol Hepatol,* 6**,** 545-55.

BARANN, M., DILGER, J. P., BONISCH, H., GOTHERT, M., DYBEK, A. & URBAN, B. W. 2000. Inhibition of 5-HT3 receptors by propofol: equilibrium and kinetic measurements. *Neuropharmacology,* 39**,** 1064-74.

BARNES, N. M. & SHARP, T. 1999. A review of central 5-HT receptors and their function. *Neuropharmacology,* 38**,** 1083-1152.

BARRERA, N. P., HERBERT, P., HENDERSON, R. M., MARTIN, I. L. & EDWARDSON, J. M. 2005. Atomic force microscopy reveals the stoichiometry and subunit arrangement of 5-HT3 receptors. *Proc Natl Acad Sci U S A,* 102**,** 12595-600.

BERTRAND, D., BERTRAND, S., CASSAR, S., GUBBINS, E., LI, J. & GOPALAKRISHNAN, M. 2008. Positive Allosteric Modulation of the alpha7 Nicotinic Acetylcholine Receptor: Ligand Interactions with Distinct Binding Sites and Evidence for a Prominent Role of the M2-M3 Segment. *Mol Pharmacol,* 74**,** 1407-1416.

BIRNBOIM, H. C. & DOLY, J. 1979. A rapid alkaline extraction procedure for screening recombinant plasmid DNA. *Nucleic Acids Res,* 7**,** 1513-23.

BLONDEL, O., GASTINEAU, M., DAHMOUNE, Y., LANGLOIS, M. & FISCHMEISTER, R. 1998. Cloning, expression, and pharmacology of four human 5-hydroxytryptamine 4 receptor isoforms produced by alternative splicing in the carboxyl terminus. *J Neurochem,* 70**,** 2252-61.

BONHAUS, D. W., BACH, C., DESOUZA, A., SALAZAR, F. H., MATSUOKA, B. D., ZUPPAN, P., CHAN, H. W. & EGLEN, R. M. 1995. The pharmacology and distribution of human 5-hydroxytryptamine2B (5-HT2B) receptor gene products: comparison with 5-HT2A and 5-HT2C receptors. *Br J Pharmacol,* 115**,** 622-8.

BOURSON, A., KAPPS, V., ZWINGELSTEIN, C., RUDLER, A., BOESS, F. G. & SLEIGHT, A. J. 1997. Correlation between 5-HT7 receptor affinity and protection

against sound-induced seizures in DBA/2J mice. *Naunyn Schmiedebergs Arch Pharmacol,* 356**,** 820-6.

BRADLEY, P. B., ENGEL, G., FENIUK, W., FOZARD, J. R., HUMPHREY, P. P., MIDDLEMISS, D. N., MYLECHARANE, E. J., RICHARDSON, B. P. & SAXENA, P. R. 1986. Proposals for the classification and nomenclature of functional receptors for 5-hydroxytryptamine. *Neuropharmacology,* 25**,** 563-76.

BREJC, K., VAN DIJK, W. J., KLAASSEN, R. V., SCHUURMANS, M., VAN DER OOST, J., SMIT, A. B. & SIXMA, T. K. 2001. Crystal structure of an ACh-binding protein reveals the ligand-binding domain of nicotinic receptors. *Nature,* 411**,** 269-76.

BROWN, A. M., HOPE, A. G., LAMBERT, J. J. & PETERS, J. A. 1998. Ion permeation and conduction in a human recombinant 5-HT3 receptor subunit (h5-HT3A). *J Physiol,* 507 (Pt 3)**,** 653-65.

BRUINVELS, A. T., LANDWEHRMEYER, B., GUSTAFSON, E. L., DURKIN, M. M., MENGOD, G., BRANCHEK, T. A., HOYER, D. & PALACIOS, J. M. 1994. Localization of 5-HT1B, 5-HT1D alpha, 5-HT1E and 5-HT1F receptor messenger RNA in rodent and primate brain. *Neuropharmacology,* 33**,** 367-86.

BUCHHEIT, K.-H., ENGEL, G., MUTSCHLER, E. & RICHARDSON, B. 1985. Study of the contractile effect of 5-hydroxytryptamine (5-HT) in the isolated longitudinal muscle strip from guinea-pig ileum. *Naunyn-Schmiedeberg's Archives of Pharmacology,* 329**,** 36-41.

CARTER, D., CHAMPNEY, M., HWANG, B. & EGLEN, R. M. 1995. Characterization of a postjunctional 5-HT receptor mediating relaxation of guinea-pig isolated ileum. *Eur J Pharmacol,* 280**,** 243-50.

CHANG, L., TONG, K. & AMEEN, V. 2010. Ischemic colitis and complications of constipation associated with the use of alosetron under a risk management plan: clinical characteristics, outcomes, and incidences. *Am J Gastroenterol,* 105**,** 866-75.

CHEN, J. J., LI, Z., PAN, H., MURPHY, D. L., TAMIR, H., KOEPSELL, H. & GERSHON, M. D. 2001. Maintenance of serotonin in the intestinal mucosa and ganglia of mice that lack the high-affinity serotonin transporter: Abnormal intestinal motility and the expression of cation transporters. *J Neurosci,* 21**,** 6348-61.

CHEN, K., YANG, W., GRIMSBY, J. & SHIH, J. C. 1992. The human 5-HT2 receptor is encoded by a multiple intron-exon gene. *Brain Res Mol Brain Res,* 14**,** 20-6.

CHOI, J. S., CHOI, B. H., AHN, H. S., KIM, M. J., RHIE, D. J., YOON, S. H., MIN, D. S., JO, Y. H., KIM, M. S., SUNG, K. W. & HAHN, S. J. 2003. Mechanism of block by

fluoxetine of 5-hydroxytryptamine3 (5-HT3)-mediated currents in NCB-20 neuroblastoma cells. *Biochem Pharmacol,* 66**,** 2125-32.

CLAEYSEN, S., FAYE, P., SEBBEN, M., LEMAIRE, S., BOCKAERT, J., DUMUIS, A. & TAVIAUX, S. 1997. Assignment of 5-hydroxytryptamine receptor (HTR4) to human chromosome 5 bands q31-->q33 by in situ hybridization. *Cytogenet Cell Genet,* 78**,** 133-4.

CONN, P. J., SANDERS-BUSH, E., HOFFMAN, B. J. & HARTIG, P. R. 1986. A unique serotonin receptor in choroid plexus is linked to phosphatidylinositol turnover. *Proc Natl Acad Sci U S A,* 83**,** 4086-8.

CONNOLLY, C. N. 2011. 2Bs or not 2Bs: that is the question. *J Physiol,* 589**,** 4085-4086.

CORRINGER, P. J., BERTRAND, S., BOHLER, S., EDELSTEIN, S. J., CHANGEUX, J. P. & BERTRAND, D. 1998. Critical elements determining diversity in agonist binding and desensitization of neuronal nicotinic acetylcholine receptors. *J Neurosci,* 18**,** 648-57.

CUTRER, F. M., YU, X.-J., AYATA, G., MOSKOWITZ, M. A. & WAEBER, C. 1999. Effects of PNU-109,291, a selective 5-HT1D receptor agonist, on electrically induced dural plasma extravasation and capsaicin-evoked c-fos immunoreactivity within trigeminal nucleus caudalis. *Neuropharmacology,* 38**,** 1043-1053.

DAHM, R. 2008. Discovering DNA: Friedrich Miescher and the early years of nucleic acid research. *Human Genetics,* 122**,** 565-581.

DAVIES, P. A. 2011. Allosteric modulation of the 5-HT(3) receptor. *Curr Opin Pharmacol,* 11**,** 75-80.

DAVIES, P. A., PISTIS, M., HANNA, M. C., PETERS, J. A., LAMBERT, J. J., HALES, T. G. & KIRKNESS, E. F. 1999. The 5-HT3B subunit is a major determinant of serotonin-receptor function. *Nature,* 397**,** 359-63.

DERKACH, V., SURPRENANT, A. & NORTH, R. A. 1989. 5-HT3 receptors are membrane ion channels. *Nature,* 339**,** 706-9.

EISELÉ, J. L., BERTRAND, S., GALZI, J. L., DEVILLERS-THIÉRY, A., CHANGEUX, J. P. & BERTRAND, D. 1993. Chimaeric nicotinic-serotonergic receptor combines distinct ligand binding and channel specificities. *Nature,* 366**,** 479-83.

FAN, P. 1994. Effects of antidepressants on the inward current mediated by 5-HT3 receptors in rat nodose ganglion neurones. *Br J Pharmacol,* 112**,** 741-4.

FDA. 2012. *Lotronex (alosetron hydrochloride) Information* [Online]. Available: www.fda.gov [Accessed 4 August 2014].

FILIP, M. & BADER, M. 2009. Overview on 5-HT receptors and their role in physiology and pathology of the central nervous system. *Pharmacol Rep,* 61**,** 761-77.

FOZARD, J. R. 1984. MDL 72222: a potent and highly selective antagonist at neuronal 5-hydroxytryptamine receptors. *Naunyn Schmiedebergs Arch Pharmacol,* 326**,** 36-44.

GADDUM, J. H. & PICARELLI, Z. P. 1957. Two kinds of tryptamine receptor. *Br J Pharmacol Chemother,* 12**,** 323-8.

GELERNTER, J., RAO, P. A., PAULS, D. L., HAMBLIN, M. W., SIBLEY, D. R. & KIDD, K. K. 1995. Assignment of the 5HT7 receptor gene (HTR7) to chromosome 10q and exclusion of genetic linkage with Tourette syndrome. *Genomics,* 26**,** 207-9.

GERSHON, M. D. & TACK, J. 2007. The Serotonin Signaling System: From Basic Understanding To Drug Development for Functional GI Disorders. *Gastroenterology,* 132**,** 397-414.

GLENNON, R. A. 1990. Do classical hallucinogens act as 5-HT2 agonists or antagonists? *Neuropsychopharmacology,* 3**,** 509-17.

GOODFELLOW, N. M., BAILEY, C. D. & LAMBE, E. K. 2012. The native serotonin 5-HT(5A) receptor: electrophysiological characterization in rodent cortex and 5-HT(1A)-mediated compensatory plasticity in the knock-out mouse. *J Neurosci,* 32**,** 5804-9.

GRAILHE, R., GRABTREE, G. W. & HEN, R. 2001. Human 5-HT(5) receptors: the 5-HT(5A) receptor is functional but the 5-HT(5B) receptor was lost during mammalian evolution. *Eur J Pharmacol,* 418**,** 157-67.

GRONLIEN, J. H., WEEN, H., THORIN-HAGENE, K., CASSAR, S., LI, J., BRIGGS, C. A., GOPALAKRISHNAN, M. & MALYSZ, J. 2010. Importance of M2-M3 loop in governing properties of genistein at the alpha7 nicotinic acetylcholine receptor inferred from alpha7/5-HT3A chimera. *Eur J Pharmacol,* 647**,** 37-47.

GUDELSKY, G. A., KOENIG, J. I. & MELTZER, H. Y. 1986. Thermoregulatory responses to serotonin (5-HT) receptor stimulation in the rat. Evidence for opposing roles of 5-HT2 and 5-HT1A receptors. *Neuropharmacology,* 25**,** 1307-13.

GUSCOTT, M., BRISTOW, L. J., HADINGHAM, K., ROSAHL, T. W., BEER, M. S., STANTON, J. A., BROMIDGE, F., OWENS, A. P., HUSCROFT, I., MYERS, J., RUPNIAK, N. M., PATEL, S., WHITING, P. J., HUTSON, P. H., FONE, K. C., BIELLO, S. M., KULAGOWSKI, J. J. & MCALLISTER, G. 2005. Genetic knockout

and pharmacological blockade studies of the 5-HT7 receptor suggest therapeutic potential in depression. *Neuropharmacology,* 48**,** 492-502.

HANSEN, M. B. & SKADHAUGE, E. 1997. Signal Transduction Pathways for Serotonin as an Intestinal Secretagogue. *Comparative Biochemistry and Physiology Part A: Physiology,* 118**,** 283-290.

HARDISTY, R. S., RS 1955. 5-Hydroxytryptamine in normal human platelets. *J Physiol.,* 130**,** 711-20.

HASSAINE, G., DELUZ, C., GRASSO, L., WYSS, R., TOL, M. B., HOVIUS, R., GRAFF, A., STAHLBERG, H., TOMIZAKI, T., MOREAU, C., LI, X., POITEVIN, F., VOGEL, H. & NURY, H. 2014. X-ray structure of the mouse serotonin 5-HT3 receptor. *Nature,* 512**,** 276.

HASSELL, A. M., AN, G., BLEDSOE, R. K., BYNUM, J. M., CARTER III, H. L., DENG, S. J., GAMPE, R. T., GRISARD, T. E., MADAUSS, K. P., NOLTE, R. T., ROCQUE, W. J., WANG, L., WEAVER, K. L., WILLIAMS, S. P., WISELY, G. B., XU, R. & SHEWCHUK, L. M. 2007. Crystallization of protein-ligand complexes. *Acta Crystallogr D Biol Crystallogr,* 63**,** 72-79.

HEISLER, L. K., CHU, H. M., BRENNAN, T. J., DANAO, J. A., BAJWA, P., PARSONS, L. H. & TECOTT, L. H. 1998. Elevated anxiety and antidepressant-like responses in serotonin 5-HT1A receptor mutant mice. *Proc Natl Acad Sci U S A,* 95**,** 15049-54.

HOUGHTON, L. A., ATKINSON, W., LOCKHART, C., WHORWELL, P. J. & KEEVIL, B. 2007. Sigmoid-colonic motility in health and irritable bowel syndrome: a role for 5-hydroxytryptamine. *Neurogastroenterol Motil,* 19**,** 724-31.

HOYER, D., CLARKE, D. E., FOZARD, J. R., HARTIG, P. R., MARTIN, G. R., MYLECHARANE, E. J., SAXENA, P. R. & HUMPHREY, P. P. 1994. International Union of Pharmacology classification of receptors for 5-hydroxytryptamine (Serotonin). *Pharmacol Rev,* 46**,** 157-203.

HOYER, D., HANNON, J. P. & MARTIN, G. R. 2002. Molecular, pharmacological and functional diversity of 5-HT receptors. *Pharmacol Biochem Behav,* 71**,** 533-54.

HOYER, D. & MIDDLEMISS, D. N. 1989. Species differences in the pharmacology of terminal 5-HT autoreceptors in mammalian brain. *Trends Pharmacol Sci,* 10**,** 130-2.

HULISZ, D. 2004. The burden of illness of irritable bowel syndrome: current challenges and hope for the future. *J Manag Care Pharm,* 10**,** 299-309.

JØRGENSEN, H., KJÆR, A., WARBERG, J. & KNIGGE, U. 2001. Differential Effect of Serotonin 5-HT$_{1A}$ Receptor Antagonists on the Secretion of Corticotropin and Prolactin. *Neuroendocrinology,* 73**,** 322-333.

KELLEY, S. P., DUNLOP, J. I., KIRKNESS, E. F., LAMBERT, J. J. & PETERS, J. A. 2003. A cytoplasmic region determines single-channel conductance in 5-HT3 receptors. *Nature,* 424**,** 321-4.

KENNETT, G. A., BRIGHT, F., TRAIL, B., BAXTER, G. S. & BLACKBURN, T. P. 1996. Effects of the 5-HT2B receptor agonist, BW 723C86, on three rat models of anxiety. *Br J Pharmacol,* 117**,** 1443-8.

KESTERS, D., THOMPSON, A. J., BRAMS, M., VAN ELK, R., SPURNY, R., GEITMANN, M., VILLALGORDO, J. M., GUSKOV, A., DANIELSON, U. H., LUMMIS, S. C., SMIT, A. B. & ULENS, C. 2013. Structural basis of ligand recognition in 5-HT3 receptors. *EMBO Rep,* 14**,** 49-56.

KILPATRICK, G. J., JONES, B. J. & TYERS, M. B. 1987. Identification and distribution of 5-HT3 receptors in rat brain using radioligand binding. *Nature,* 330**,** 746-8.

KITAMURA, O., WEE, S., SPECIO, S. E., KOOB, G. F. & PULVIRENTI, L. 2006. Escalation of methamphetamine self-administration in rats: a dose-effect function. *Psychopharmacology (Berl),* 186**,** 48-53.

KOEK, W., JACKSON, A. & COLPAERT, F. C. 1992. Behavioral pharmacology of antagonists at 5-HT2/5-HT1C receptors. *Neurosci Biobehav Rev,* 16**,** 95-105.

KOHEN, R., METCALF, M. A., KHAN, N., DRUCK, T., HUEBNER, K., LACHOWICZ, J. E., MELTZER, H. Y., SIBLEY, D. R., ROTH, B. L. & HAMBLIN, M. W. 1996. Cloning, Characterization, and Chromosomal Localization of a Human 5-HT6 Serotonin Receptor. *Journal of Neurochemistry,* 66**,** 47-56.

KOOYMAN, A. R., VAN HOOFT, J. A., VANDERHEIJDEN, P. M. L. & VIJVERBERG, H. P. M. 1994. Competitive and non-competitive effects of 5-hydroxyindole on 5-HT3 receptors in N1E-115 neuroblastoma cells. *British Journal of Pharmacology,* 112**,** 541-546.

KRACUN, S., HARKNESS, P. C., GIBB, A. J. & MILLAR, N. S. 2008. Influence of the M3-M4 intracellular domain upon nicotinic acetylcholine receptor assembly, targeting and function. *Br J Pharmacol,* 153**,** 1474-1484.

LAMBERT, J. J., PETERS, J. A., HALES, T. G. & DEMPSTER, J. 1989. The properties of 5-HT3 receptors in clonal cell lines studied by patch-clamp techniques. *Br J Pharmacol,* 97**,** 27-40.

LANGER, S. Z., BRILEY, M. S., RAISMAN, R., HENRY, J. F. & MORSELLI, P. L. 1980. Specific 3H-imipramine binding in human platelets. *Naunyn-Schmiedeberg's Archives of Pharmacology,* 313**,** 189-194.

LEVY, F. O., HOLTGREVE-GREZ, H., TASKEN, K., SOLBERG, R., RIED, T. & GUDERMANN, T. 1994. Assignment of the gene encoding the 5-HT1E serotonin receptor (S31) (locus HTR1E) to human chromosome 6q14-q15. *Genomics,* 22**,** 637-40.

LISI, D. M. 2002. Lotronex withdrawal. *Arch Intern Med,* 162**,** 101.

LOPEZ-GIMENEZ, J. F., MENGOD, G., PALACIOS, J. M. & VILARO, M. T. 1997. Selective visualization of rat brain 5-HT2A receptors by autoradiography with [3H]MDL 100,907. *Naunyn Schmiedebergs Arch Pharmacol,* 356**,** 446-54.

LOVENBERG, T. W., BARON, B. M., DE LECEA, L., MILLER, J. D., PROSSER, R. A., REA, M. A., FOYE, P. E., RACKE, M., SLONE, A. L., SIEGEL, B. W. & ET AL. 1993. A novel adenylyl cyclase-activating serotonin receptor (5-HT7) implicated in the regulation of mammalian circadian rhythms. *Neuron,* 11**,** 449-58.

LUMMIS, S. C. 2012. 5-HT3 Receptors. *J Biol Chem,* 287.

MARTIN, G. R. & HUMPHREY, P. P. 1994. Receptors for 5-hydroxytryptamine: current perspectives on classification and nomenclature. *Neuropharmacology,* 33**,** 261-73.

MATSUEDA, K., HARASAWA, S., HONGO, M., HIWATASHI, N. & SASAKI, D. 2008. A randomized, double-blind, placebo-controlled clinical trial of the effectiveness of the novel serotonin type 3 receptor antagonist ramosetron in both male and female Japanese patients with diarrhea-predominant irritable bowel syndrome. *Scand J Gastroenterol,* 43**,** 1202-11.

MENESES, A., MANUEL-APOLINAR, L., CASTILLO, C. & CASTILLO, E. 2007. Memory consolidation and amnesia modify 5-HT6 receptors expression in rat brain: an autoradiographic study. *Behav Brain Res,* 178**,** 53-61.

MIALET, J., DAHMOUNE, Y., LEZOUALC'H, F., BERQUE-BESTEL, I., EFTEKHARI, P., HOEBEKE, J., SICSIC, S., LANGLOIS, M. & FISCHMEISTER, R. 2000. Exploration of the ligand binding site of the human 5-HT(4) receptor by site-directed mutagenesis and molecular modeling. *Br J Pharmacol,* 130**,** 527-38.

MIDDLEMISS, D. N. & FOZARD, J. R. 1983. 8-Hydroxy-2-(di-n-propylamino)-tetralin discriminates between subtypes of the 5-HT1 recognition site. *Eur J Pharmacol,* 90**,** 151-3.

MINER, W. D. & SANGER, G. J. 1986. Inhibition of cisplatin-induced vomiting by selective 5-hydroxytryptamine M-receptor antagonism. *Br J Pharmacol,* 88**,** 497-9.

MIYAZAWA, A., FUJIYOSHI, Y. & UNWIN, N. 2003. Structure and gating mechanism of the acetylcholine receptor pore. *Nature,* 423**,** 949-55.

MONSMA, F. J., JR., SHEN, Y., WARD, R. P., HAMBLIN, M. W. & SIBLEY, D. R. 1993. Cloning and expression of a novel serotonin receptor with high affinity for tricyclic psychotropic drugs. *Mol Pharmacol,* 43**,** 320-7.

MORALES, M., BATTENBERG, E. & BLOOM, F. E. 1998. Distribution of neurons expressing immunoreactivity for the 5HT3 receptor subtype in the rat brain and spinal cord. *J Comp Neurol,* 402**,** 385-401.

MURPHY, D. A., AM; WICHEMS, CH; LI, Q; TOHDA, M; GREENBERG, B 1998. Brain serotonin neurotransmission: an overview and update with an emphasis on serotonin subsystem heterogeneity, multiple receptors, interactions with other neurotransmitter systems, and consequent implications for understanding the actions of serotonergic drugs. . *J Clin Psychiatry,* 59**,** 4-12.

NEWMAN, A. S., BATIS, N., GRAFTON, G., CAPUTO, F., BRADY, C. A., LAMBERT, J. J., PETERS, J. A., GORDON, J., BRAIN, K. L., POWELL, A. D. & BARNES, N. M. 2013. 5-Chloroindole: a potent allosteric modulator of the 5-HT3 receptor. *British Journal of Pharmacology,* 169**,** 1228-1238.

NIESLER, B., KAPELLER, J., HAMMER, C. & RAPPOLD, G. 2008. Serotonin type 3 receptor genes: HTR3A, B, C, D, E. *Pharmacogenomics,* 9**,** 501-4.

NIESLER, B., WALSTAB, J., COMBRINK, S., MOLLER, D., KAPELLER, J., RIETDORF, J., BONISCH, H., GOTHERT, M., RAPPOLD, G. & BRUSS, M. 2007. Characterization of the novel human serotonin receptor subunits 5-HT3C,5-HT3D, and 5-HT3E. *Mol Pharmacol,* 72**,** 8-17.

PAUWELS, P. J. 1997. 5-HT 1B/D receptor antagonists. *Gen Pharmacol,* 29**,** 293-303.

PAZOS, A. & PALACIOS, J. M. 1985. Quantitative autoradiographic mapping of serotonin receptors in the rat brain. I. Serotonin-1 receptors. *Brain Research,* 346**,** 205-230.

RAPPORT, M. G., AA; PAGE, IH 1947. Purification of the substance which is responsible for the vasoconstrictor activity of serum. *Fed Proc.,* 6.

ROBERTS, C., WATSON, J., PRICE, G. W. & MIDDLEMISS, D. N. 2001. SB-236057-A: a selective 5-HT1B receptor inverse agonist. *CNS Drug Rev,* 7**,** 433-44.

RUAT, M., TRAIFFORT, E., ARRANG, J. M., TARDIVEL-LACOMBE, J., DIAZ, J., LEURS, R. & SCHWARTZ, J. C. 1993. A novel rat serotonin (5-HT6) receptor: molecular cloning, localization and stimulation of cAMP accumulation. *Biochem Biophys Res Commun,* 193**,** 268-76.

SANGER, F. & COULSON, A. R. 1975. A rapid method for determining sequences in DNA by primed synthesis with DNA polymerase. *Journal of Molecular Biology,* 94**,** 441-448.

SAUDOU, F. & HEN, R. 1994. 5-Hydroxytryptamine receptor subtypes in vertebrates and invertebrates. *Neurochemistry International,* 25**,** 503-532.

SCHANEN, N. C., SCHERER, S. W., TSUI, L. C. & FRANCKE, U. 1996. Assignment of the 5-hydroxytryptamine (serotonin) receptor 5A gene (HTR5A) to human chromosome band 7q36.1. *Cytogenet Cell Genet,* 72**,** 187-8.

SHELDON, P. W. & AGHAJANIAN, G. K. 1991. Excitatory responses to serotonin (5-HT) in neurons of the rat piriform cortex: evidence for mediation by 5-HT1C receptors in pyramidal cells and 5-HT2 receptors in interneurons. *Synapse,* 9**,** 208-18.

SIKANDER, A., RANA, S. V. & PRASAD, K. K. 2009. Role of serotonin in gastrointestinal motility and irritable bowel syndrome. *Clinica Chimica Acta,* 403**,** 47-55.

SLEIGHT, A. J., BOESS, F. G., BOS, M., LEVET-TRAFIT, B., RIEMER, C. & BOURSON, A. 1998. Characterization of Ro 04-6790 and Ro 63-0563: potent and selective antagonists at human and rat 5-HT6 receptors. *Br J Pharmacol,* 124**,** 556-62.

SPILLER, R. C. 2011. Targeting the 5-HT3 receptor in the treatment of irritable bowel syndrome. *Current Opinion in Pharmacology,* 11**,** 68-74.

STOWE, R. L. & BARNES, N. M. 1998. Selective labelling of 5-HT7 receptor recognition sites in rat brain using [3H]5-carboxamidotryptamine. *Neuropharmacology,* 37**,** 1611-9.

TALLEY, N. J., PHILLIPS, S. F., HADDAD, A., MILLER, L. J., TWOMEY, C., ZINSMEISTER, A. R., MACCARTY, R. L. & CIOCIOLA, A. 1990. GR 38032F (ondansetron), a selective 5HT3 receptor antagonist, slows colonic transit in healthy man. *Dig Dis Sci,* 35**,** 477-80.

THOMPSON, A. J. & LUMMIS, S. C. 2003. A single ring of charged amino acids at one end of the pore can control ion selectivity in the 5-HT3 receptor. *Br J Pharmacol,* 140**,** 359-65.

THOMPSON, A. J. & LUMMIS, S. C. 2006. 5-HT3 receptors. *Curr Pharm Des,* 12**,** 3615-30.

THOMPSON, A. J. & LUMMIS, S. C. 2007. The 5-HT3 receptor as a therapeutic target. *Expert Opin Ther Targets,* 11**,** 527-40.

THOMSON, A. J., PRICE, K. L. & LUMMIS, S. C. 2011. Cysteine modification reveals which subunits form the ligand binding site in human heteromeric 5-HT3AB receptors. *J Physiol.,* 589(Pt 17)**,** 4243-4257.

TUNNICLIFF, G. 1991. Molecular Basis of Buspirone's Anxiolytic Action. *Pharmacology & Toxicology,* 69**,** 149-156.

UNWIN, N. 2005. Refined structure of the nicotinic acetylcholine receptor at 4A resolution. *J Mol Biol,* 346**,** 967-89.

VANHOUTTE, P. 1991. Platelet-derived serotonin, the endothelium, and cardiovascular disease. *J Cardiovasc Pharmacol. ,* 17**,** S6-12.

XIE, E., ZHU, L., ZHAO, L. & CHANG, L. S. 1996. The human serotonin 5-HT2C receptor: complete cDNA, genomic structure, and alternatively spliced variant. *Genomics,* 35**,** 551-61.

ZWART, R., DE FILIPPI, G., BROAD, L. M., MCPHIE, G. I., PEARSON, K. H., BALDWINSON, T. & SHER, E. 2002. 5-Hydroxyindole potentiates human alpha 7 nicotinic receptor-mediated responses and enhances acetylcholine-induced glutamate release in cerebellar slices. *Neuropharmacology,* 43**,** 374-84.